This research has been co-financed by European Union's Seventh Framework Programme (FP7-REGPOT-2012-2013-1) under grant agreement No 316165. and the European Union (European Social Fund, ESF) and Greek national funds through the Operational Program "Education and Lifelong Learning" of the National Strategic Reference Framework (NSRF), under the grants schemes "Funding of proposals that have received a positive evaluation in the 3rd and 4th Call of ERC Grant Schemes"

Newton workshop: "Holography: from gravity to quantum matter"
Cambridge, 18 September 2013

The IR landscape of holography: Cohesive and fractionalised phases, insulators and bad metals.

Elias Kiritsis

CCTP University of Crete QCN APC, Paris

Bibliography

Based on ongoing work with

A. Donos (Cambridge) and B. Gouteraux, (Nordita)

and

A. Donos (Cambridge)

Plan

- Introduction
- The Wilson program and the IR landscape
- Conductors and Insulators
- Irrelevant lattices: the hyperscaling violating semi-local geometries.
- Relevant breaking: insulators and bad metals in EMD theories
- Outlook

Introduction

- Condensed matter physics is strongly driven by data

- Most of these data, beyond thermodynamics, are related to conductivities in the presence of various background fields

- They form an important package that characterises the systems under study.

- The goal is to theoretically explain this set of data.

There are however two roads to the reach the theoretical description:

• Targeted model building driven by experimental data

• Exploration of theoretical possibilities, before doing model bulding

In QFT, the second approach was pioneered by Wilson:

• Specify the symmetry

• Find all theories that are scale invariant (SITs) and respect that symmetry.

• Map the neighborhood of each SIT, by using a local chart of low dimension scaling operators, and determine the local RG flows.

• Fill in the global set of RG Flows, connecting the network of SITs.

Fixed point theories

The main "atoms" in the QFT "lego-game" are the fixed-point theories (Scale invariant Theories) for a given symmetry universality class.

• At weak coupling, such theories can be searched for perturbatively. There are VERY FEW examples beyond free-field theories.

• At strong coupling, only very special symmetries (like extended supersymmetry) or the large-N_c expansion can provide a few more examples. (2d is an exception)

♠ All in all, we know VERY FEW Scale invariant Theories in three and more dimensions.

• Since the AdS/CFT correspondence entered the game, many more became known: they are large N_c theories at strong coupling.

• Despite this, we know only a drop in the ocean of SITs.

.

- To go further and map the neighborhood of SITs, we must "solve" them.

- For the first step we need the scaling dimensions.

- For the next step we need OPE coefficients.

- Once we have them we can locally map the neighborhood and draw a flow chart.

♠ The final step , following RG a finite distance away is only possible at weak coupling and in some cases which can be argued on the basis of symmetries and other special info.

The classification of QC theories

• The program: Classification of SI theories (The Wilsonian approach in AdS/CFT).

• The strategy is to use Effective Holographic Theories (the analogue of effective FT in the holographic case) in order to explore all possible QC holographic scale invariant theories with given symmetries.

Charmousis+Gouteraux+Kim+E.K.+Meyer, '10

To do this we must

1. Select the operators expected to be important for the dynamics

2. Write an effective (gravitational) holographic action that captures the (IR) dynamics by parametrizing the IR asymptotics of interactions .

3. Find the scaling solutions describing extremal saddle points, with given symmetries. Built the $T \to 0$ bh solutions around them

4. Study the physics around each acceptable saddle point.

• This strategy has been applied sporadically so far and started bearing fruit:

• It dealt with various symmetry classes, including Poincaré invariance, Lifshitz symmetries, hyperscaling violation and more general Bianchi-type symmetries.

Charmousis+Gouteraux+Kim+E.K.+Meyer, '10
Perlmutter, '10, Gouteraux+E.K., '11
Huisje+Sachdev+Swingle, '11
Dong+Harrison+Kachru+Torroba+Wang, '11
Iizuka+Kachru+Kundu+Narayan+Sircar+Trivedi, '12
Donos+Gauntlett, '11, Donos+Gauntlett+Pantelidou, '11
Hartnoll+Huijse, '11, Hartnoll+Shaghoulian, '12, Donos+Hartnoll, '12
Iizuka+Kachru+Kundu+Narayan+Sircar+Trivedi+Wang, '12
Iizuka+Maeda, '13

Important characteristics of Saddle-points

♠ We look for QC theories at finite density (at least one U(1) global symmetry). Options:

• The SYMMETRY of the metric ($T = 0$).

Translational invariant saddle points:

$$(\theta, \mathrm{z}) - \text{Lifshitz} \qquad : \qquad ds^2 = r^\theta \left[-\frac{dt^2}{r^{2z}} + \frac{dr^2 + d\vec{x}^2}{r^2} \right]$$

Charmousis+Gouteraux+Kim+Kiritsis+Meyer, '10, Gouteraux+Kiritsis, '11, Huisje+Sachdev+Swingle, '11

hyperscaling exponent: $\theta \neq 0$ Hyperscaling violation (associated with running scalars).

Lifshitz exponent: $z \neq 1$ breaking of relativistic (conformal invariance)

• Breakdown of some translational symmetries: Bianchi classification, and by now many examples.

Iizuka+Kachru+Kundu+Narayan+Sircar+Trivedi, '12

Charge: Fractionalized vs cohesive phases

- Where is the charge located?
- Event horizons $\Leftrightarrow$ deconfined phases $\Leftrightarrow$ fractionalised dofs.

Witten, '98

- Separate contributions to the boundary charge density

Hartnoll, '11

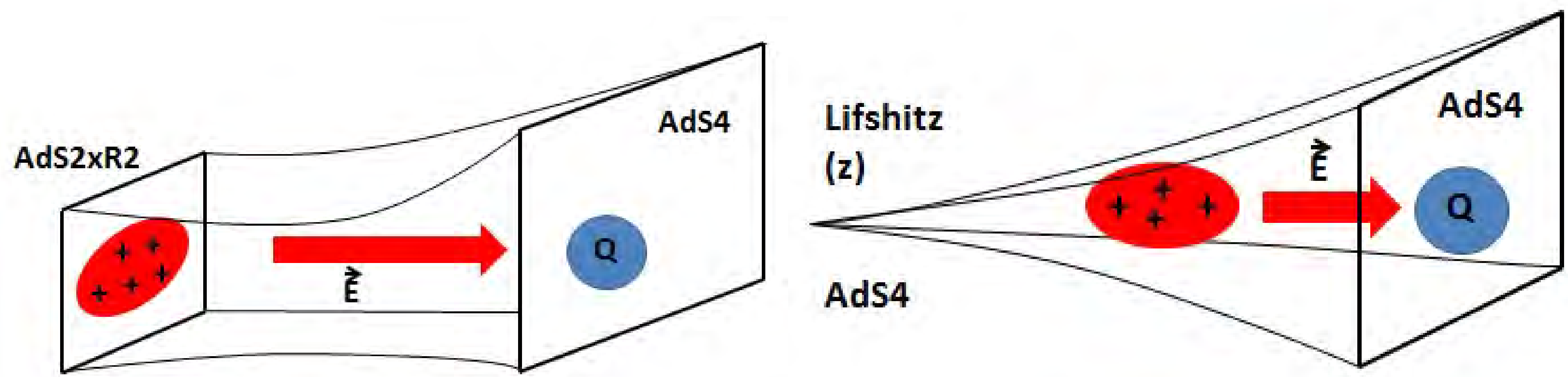

$$\textit{Fractionalised phase} \quad : \quad \lim_{r\to\infty} \int \star F \simeq Q \neq 0$$

$$\textit{Cohesive phase} \quad : \quad \lim_{r\to\infty} \int \star F \simeq 0$$

• The current in the IR can be also relevant or irrelevant.

• These four cases are independent and are controlled by two extra critical exponents.

Gouteraux, '13

• In EMD effective theories

$$S_M = M^2 \int d^4x\sqrt{-g}\left[R - \frac{1}{2}(\partial\phi)^2 + V(\phi) - \frac{Z(\phi)}{4}F^2 - \frac{W(\phi)}{2}A^2 + \frac{U(\phi)}{4}F\tilde{F}\right].$$

• (without CP violation: $U = 0$ in the IR) all scaling IR asymptotics with translation symmetry, and either broken or unbroken U(1) symmetry have been classified.

Gouteraux+Kiritsis, '11

• They are classified by four critical exponents: (z,θ) as well as the cohesion and conduction exponents, (ξ,ζ)

Gouteraux, '13

$$\int Z^* F \sim r^{\xi} \quad , \quad A_t \sim r^{\zeta-\xi-z}$$

Quantum fractionalisation transitions

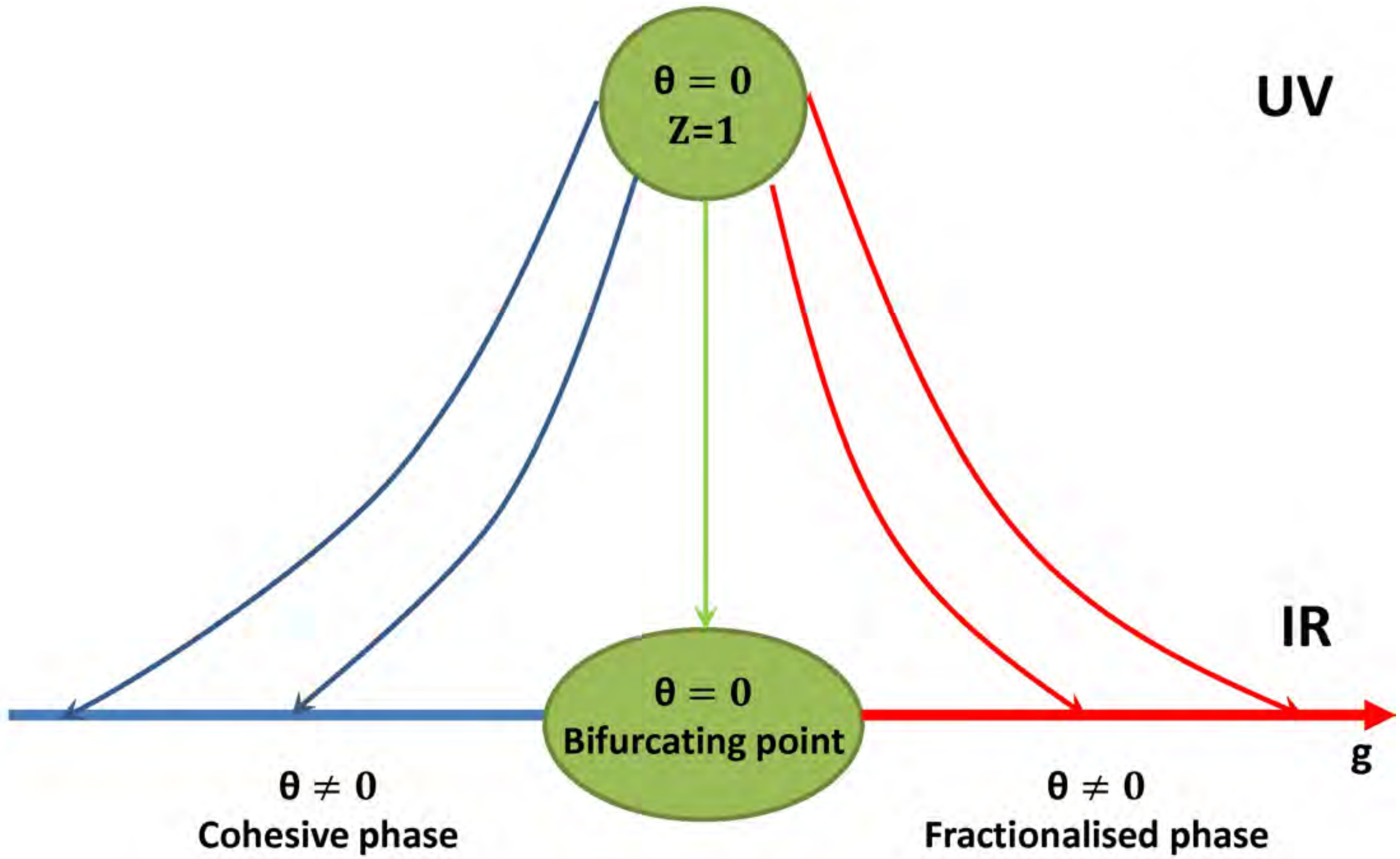

Hartnoll+Huijse'11, Adam+Crampton+Sonner+Withers '12, Goutéraux+Kiritsis '12

Scale invariant fixed point ($\theta = 0$) with a relevant deformation. To reach this point, the flow must be fine tuned. Away from the critical value, the flow picks up the relevant deformation and lands into hyperscaling violation fixed points: a quantum critical line. The line originates from an extra scaling symmetry: $\phi \to \phi + \phi_0$, $Q \to e^{\#\phi_0} Q$

Conductivity

• This is one of the most important characteristics of materials, as it is easy to be measured, and conveys a lot of information on the physics.

• It can be calculated in the linear regime from the correlators of the currents

$$\sigma_{ij}(\omega,\vec{k}) = \frac{1}{i\omega}\int d^p x dt\ e^{-i\omega t - i\vec{k}\cdot\vec{x}}\langle J_i(t,\vec{x})J_j(0,0)\rangle$$

or more generally as the (non-linear) response to an external electric field

$$J_i = \sigma_{ij}\ E_j$$

• Translational invariance and finite density imply a pole at zero frequency for the conductivity.

$$\sigma(\omega) \simeq K\left(\delta(\omega) + \frac{i}{\omega}\right) + \cdots \quad , \quad K = \frac{4\rho^2}{\varepsilon + p}$$

• Weak scattering over ions or impurities, resolves the zero frequency pole

$$\sigma(\omega) \simeq \frac{K\tau}{1 - i\omega\tau} + \cdots \quad , \quad \frac{1}{\tau} = \text{scattering rate}$$

In the limit $\tau \to \infty$ we obtain the zero frequency pole.

- This is the so-called Drude peak and defines the response of a metal at low frequencies.

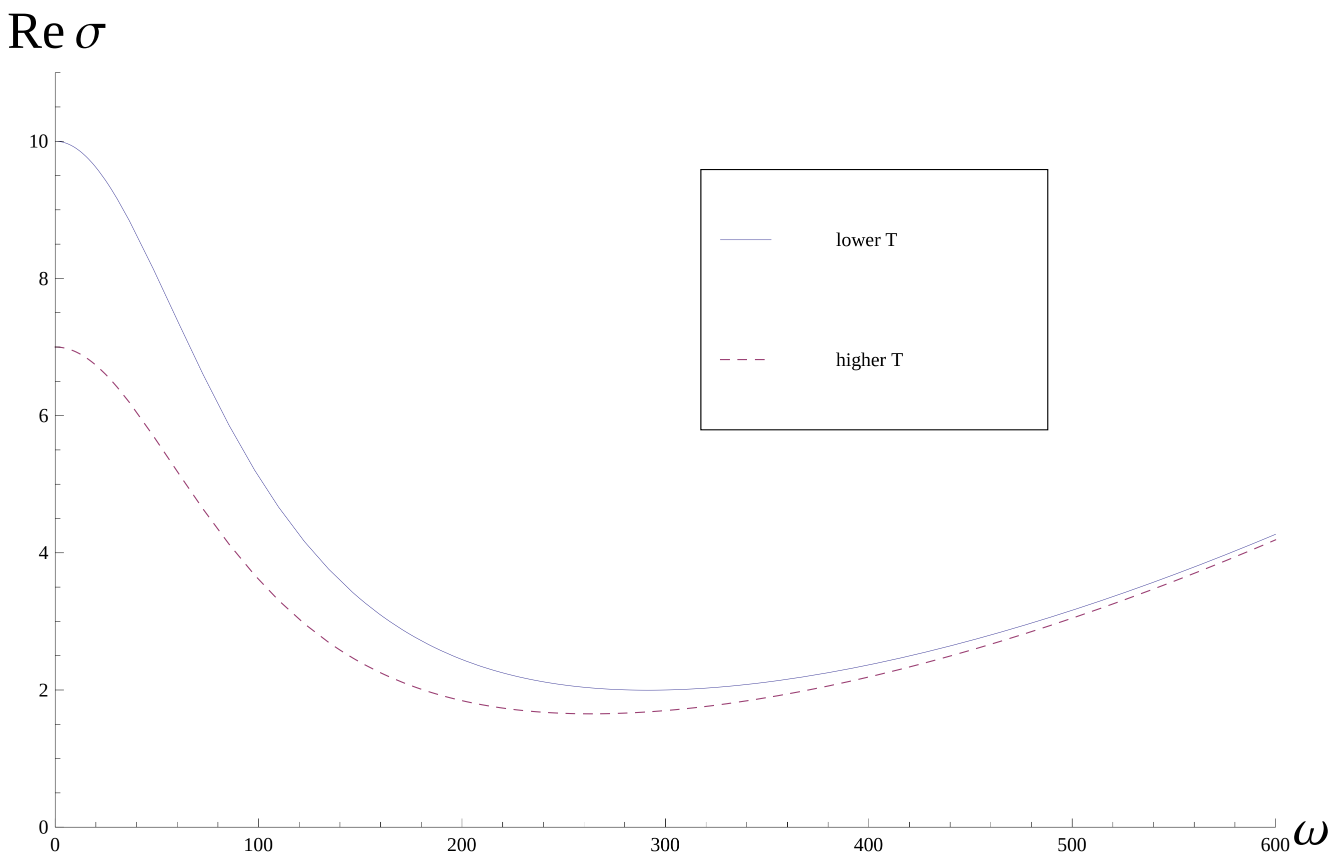

- As $T \to 0$, $\tau \to \infty$.

• A lattice of wavelength k_L breaks translation invariance, and therefore induces a non-zero scattering time τ.

• If the lattice is irrelevant in the IR, AND the translationally invariant theory is semilocal, there is a leading irrelevant operator that mediates this scattering, with dimension $\Delta(k_L)$.

• The semilocal geometries include $AdS_2 \times R^n$ and conformal variants obtained as $z \to \infty$, $\theta \to \infty$, with $\frac{z}{\theta} = \lambda$ fixed

Gouteraux+Kiritsis, '11, Huise+Sachdev+Swingle, '11

• The DC conductivity is controlled by τ and

$$\sigma_{DC} \sim T^{\Delta(k_L)} \quad , \quad \Delta(k_L) = 2\nu_- - 1$$

$$\nu_- = \frac{\lambda+1}{2\sqrt{\lambda+2}}\sqrt{\lambda + 10 + 4(\lambda+2)k_L^2\ell_{IR}^2 - 8\sqrt{1+(\lambda+2)k_L^2\ell_{IR}^2}}$$

Hartnoll+Hofman, '12, Anantua+Hartnoll+Martin+Ramirez, '12

Insulators at strong coupling

• There are two ways that a system can be insulating at T=0:

♠ Charged excitations are gapped. In that case the conductivity is non-zero only above the gap.

♠ There is no gap but the limit $\omega \to 0$ gives a vanishing conductivity.

In both cases the operator/mechanism that breaks translation invariance, is relevant in the IR.

• Gapped holographic systems are known at zero charge density, and they are in use as models of YM.

Witten, '98, Gursoy+Kiritsis+Nitti, '07, Nishioka+Ryu+Takatanagi, '10, Horowitz et al., '13

• At finite density, many saddle-points with discrete spectrum were found, in the classification of QC points in EMD Theories.

Charmousis+Gouteraux+Kiritsis+Kim+Meyer, '10, McGreevy+Balasubramanian, '10

• They have however the standard translation pole at zero frequency: They are more like conventional superconductors, with a hard gap, but without symmetry breaking.

• They are "Mott metals", and at finite temperature, they become standard metals after a first order phase transition.

Discrete current-current spectra

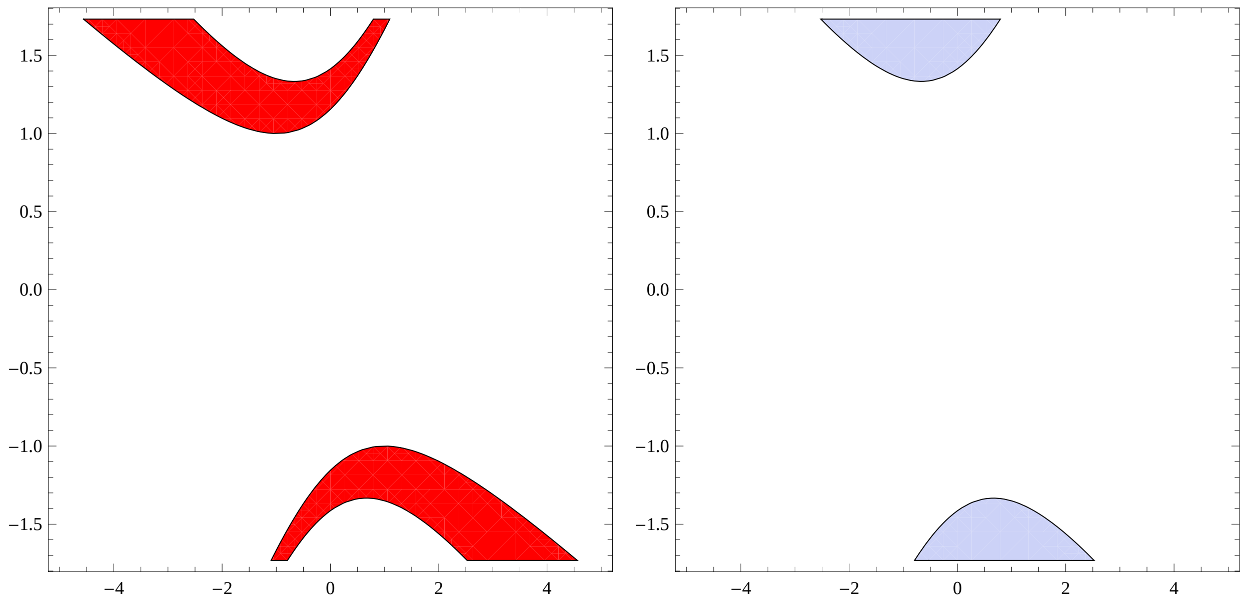

Left: The region on the $(\gamma\delta)$ plane where the IR black holes are unstable and $c > 0$. Here the extremal finite density system has a mass gap and a discrete spectrum of charged excitations, when $\Delta < 1$. Right:The region where the IR black holes are unstable, and $c < 0$. In this region the extremal finite density system has a gapless continuous spectrum at zero temperature. In both figures the horizontal axis parametrizes γ, whereas the vertical axis δ.

- An interesting problem that we are currently solving is the fate of these spectra if they are perturbed by a UV lattice.

Conductivity in semilocal geometries

• The project is to generalize the Horowitz-Santos-Tong calculation to general scaling IR geometries characterized by (θ, z) in the EMD action

With Aristos Donos

$$S_{\rm EMD} = M^2 \int d^4x \sqrt{-g} \left[R - \frac{1}{2}(\partial\phi)^2 + V(\phi) - \frac{Z(\phi)}{4} F^2 \right].$$

• We use the simplest functions that generate an RG Flow with a single UV fixed point (AdS_4) and two possible IR hyperscaling-violating scaling solutions:

$$V(\phi) = 6\frac{\left[\Delta(3-\Delta)e^{-\delta(\phi-\phi_0)} + 6\delta^2 e^{\frac{\Delta(3-\Delta)}{6\delta}(\phi-\phi_0)}\right]}{\ell^2(6\delta^2+\Delta(3-\Delta))} \quad , \quad Z(\phi) = e^{\gamma(\phi-\phi_0)}$$

in terms of ℓ, Δ, δ, ϕ_0.

• The two IR hyperscaling geometries, ($\phi - \phi_0 \lessgtr 0$) have exponents, (γ, δ), and $\left(\gamma, -\frac{\Delta(3-\Delta)}{6\delta}\right)$.

• We choose, $\gamma = -\delta$ so that we obtain a semilocal IR geometry.

Gouteraux+Kiritsis, '11

$$(z,\theta)=(\infty,-\infty) \quad , \quad -\frac{z}{\theta}=\frac{\delta^2-1}{2\delta^2}\equiv\lambda>0$$

• We choose, $\Delta=2$ and introduce sources that break translation invariance:

$$A_t(x_1)=\mu\,[1+A\cos(k_L x_1)] \quad , \quad \phi(x_1)=0$$

along with a flat boundary metric.

• The background equations are solved numerically using the DeTurk method.

• The solution corresponds to a flow between AdS_4 in the UV and a semilocal hyperscaling-violating geometry

$$ds^2=r^{-\lambda}\;ds^2_{AdS_2\times R^2}$$

• The fluctuation equations for the correlator $\langle J_1 J_1\rangle$ are solved numerically to extract the real and imaginary parts of the conductivity.

Convergence

- We have done several tests.

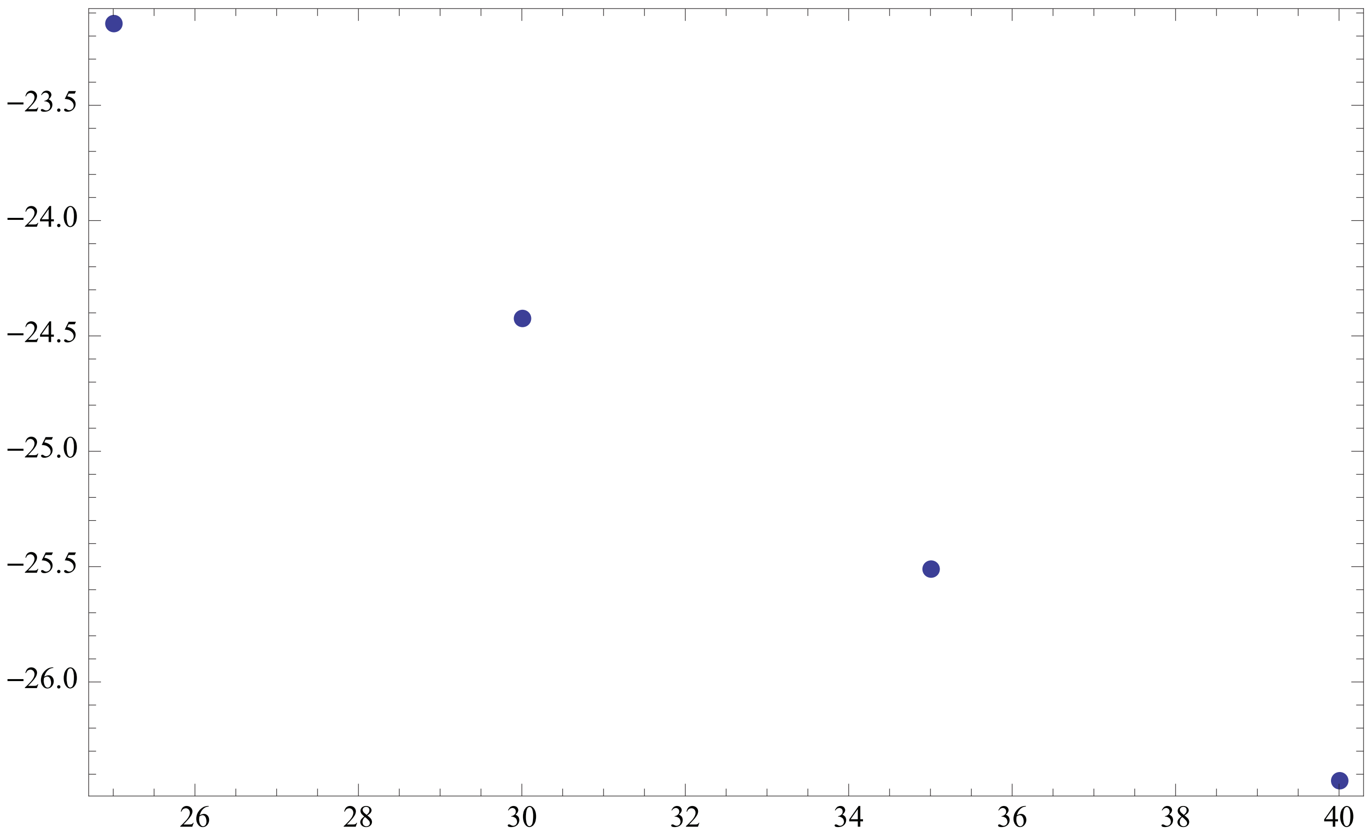

Vertical axis: $\log\left|1-\frac{S_{N+1}}{S_N}\right|$

Horizontal axis: number of points in the $N \times N$ grid

The backgrounds

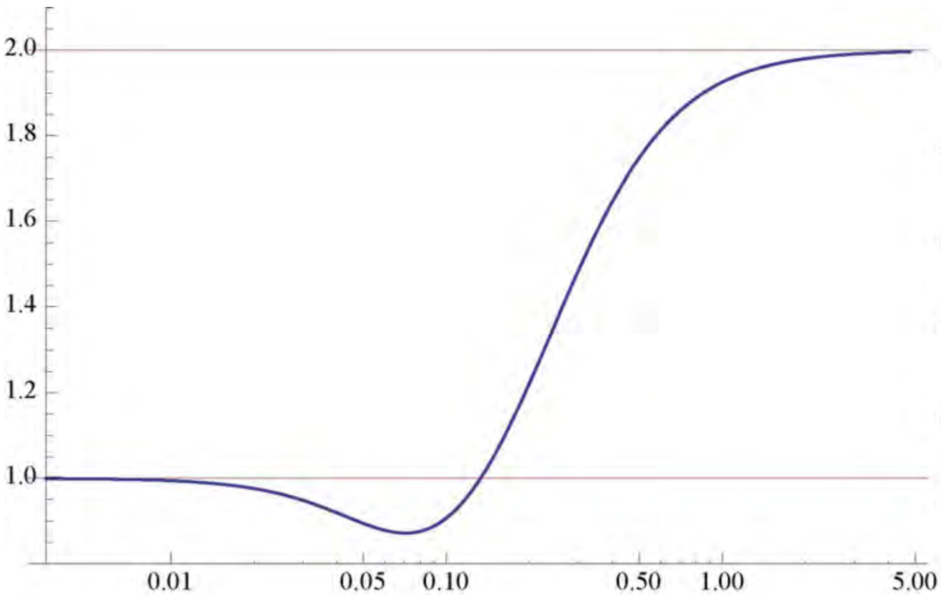

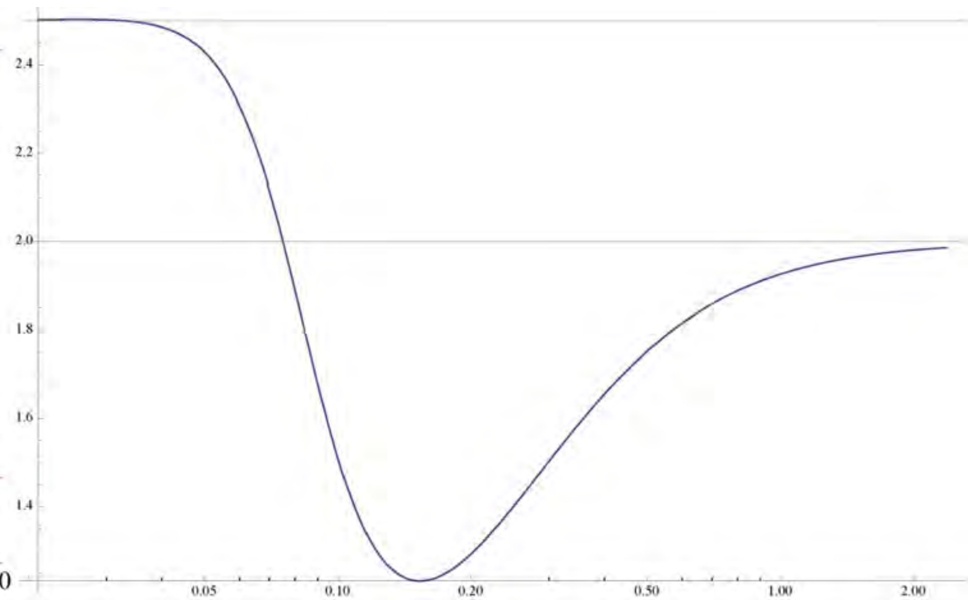

$$S_{UV} \sim T^2 \qquad S_{IR} \sim T^{\lambda}.$$

Up left: $\frac{d \log S}{d \log T}$ vs $\frac{T}{\mu}$ for $\lambda = 1$ plus the lattice.

Up right: $\frac{d \log S}{d \log T}$ vs $\frac{T}{\mu}$ for $\lambda = \frac{5}{2}$ plus the lattice.

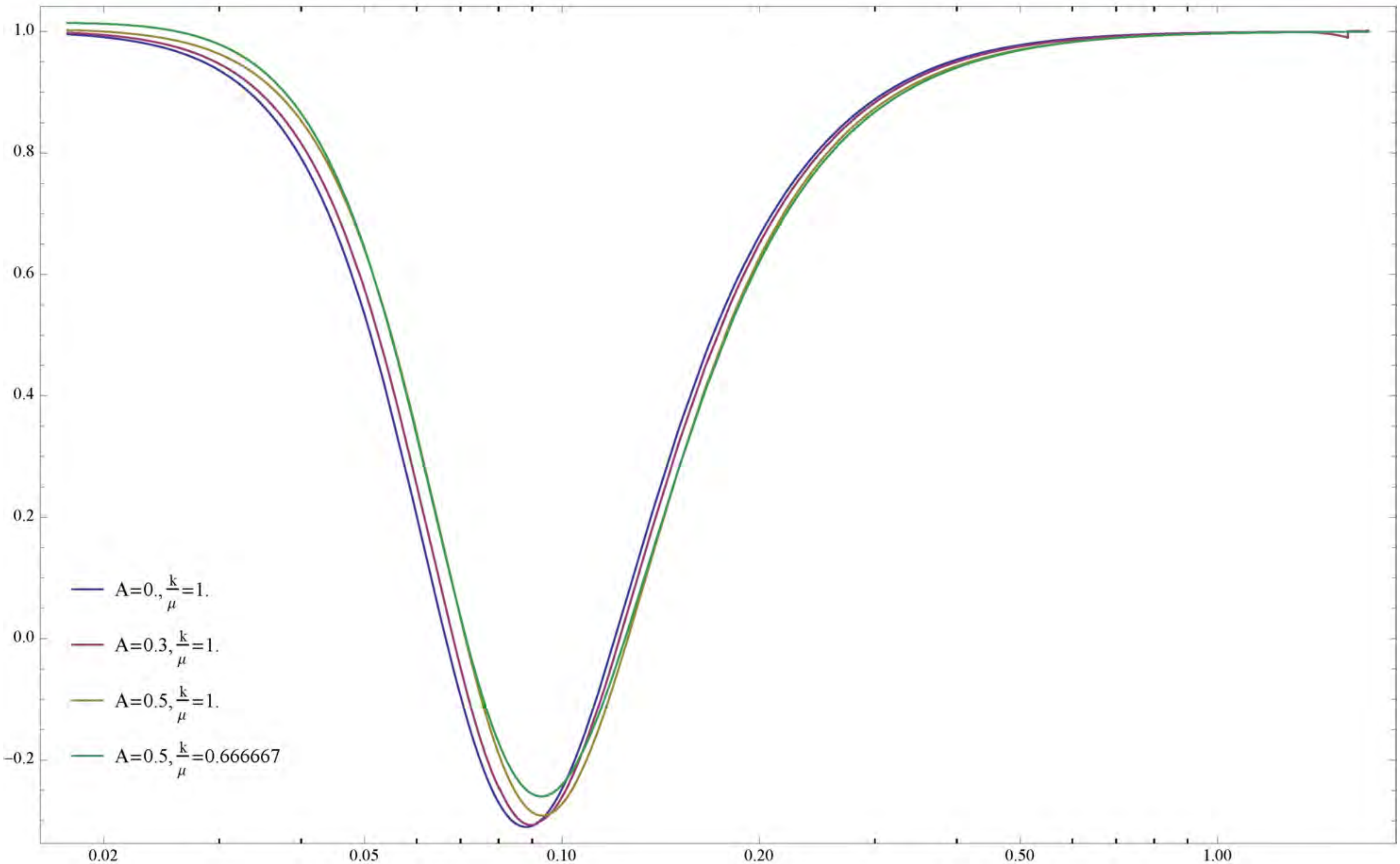

Lattice dependence of the entropy ($\lambda = 1$)

IR regime, as function of $\frac{T}{\mu}$.

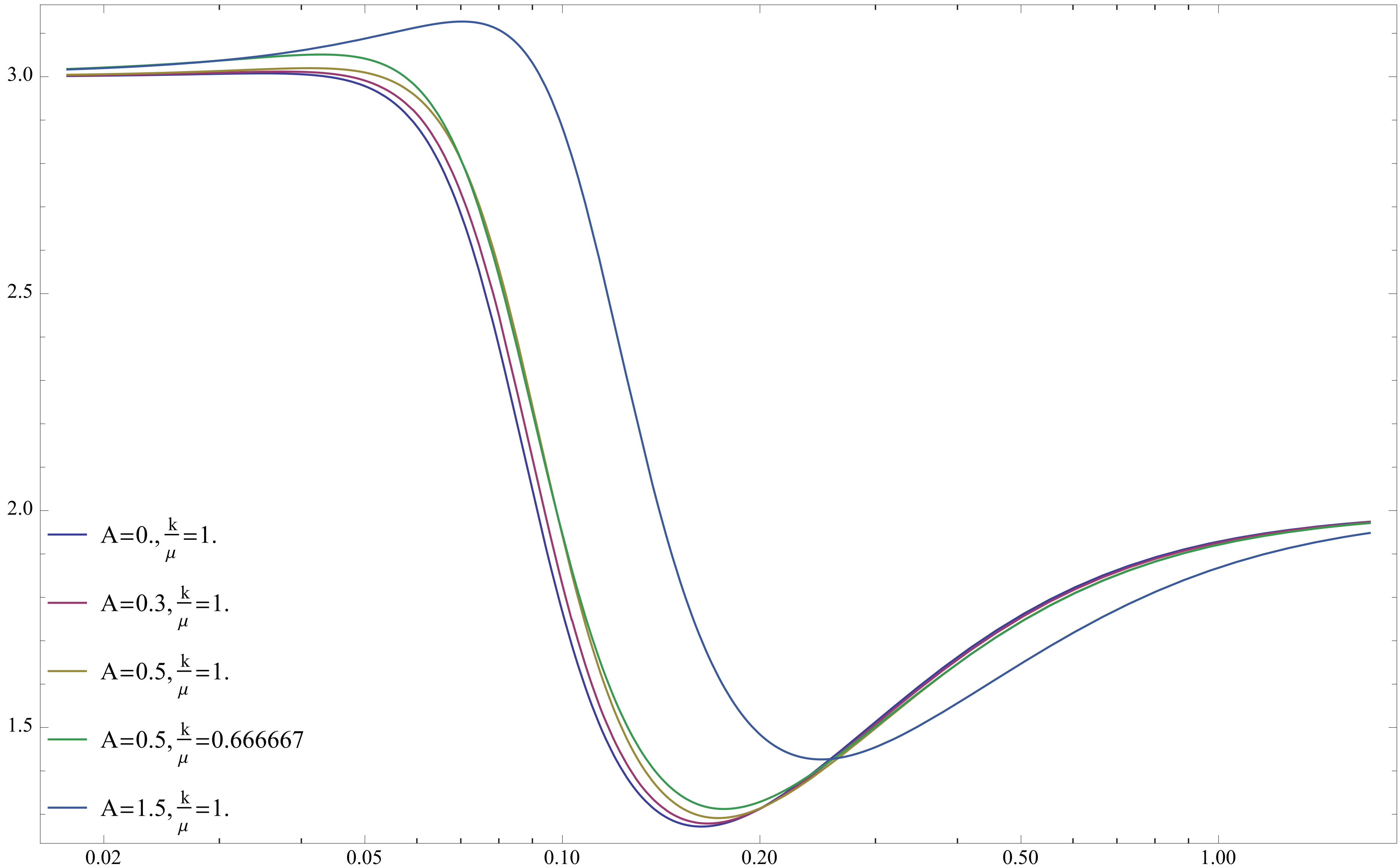

Lattice dependence of the entropy ($\lambda = 3$)

IR regime, as function of $\frac{T}{\mu}$.

AC Conductivity: $\lambda = \frac{3}{2}$

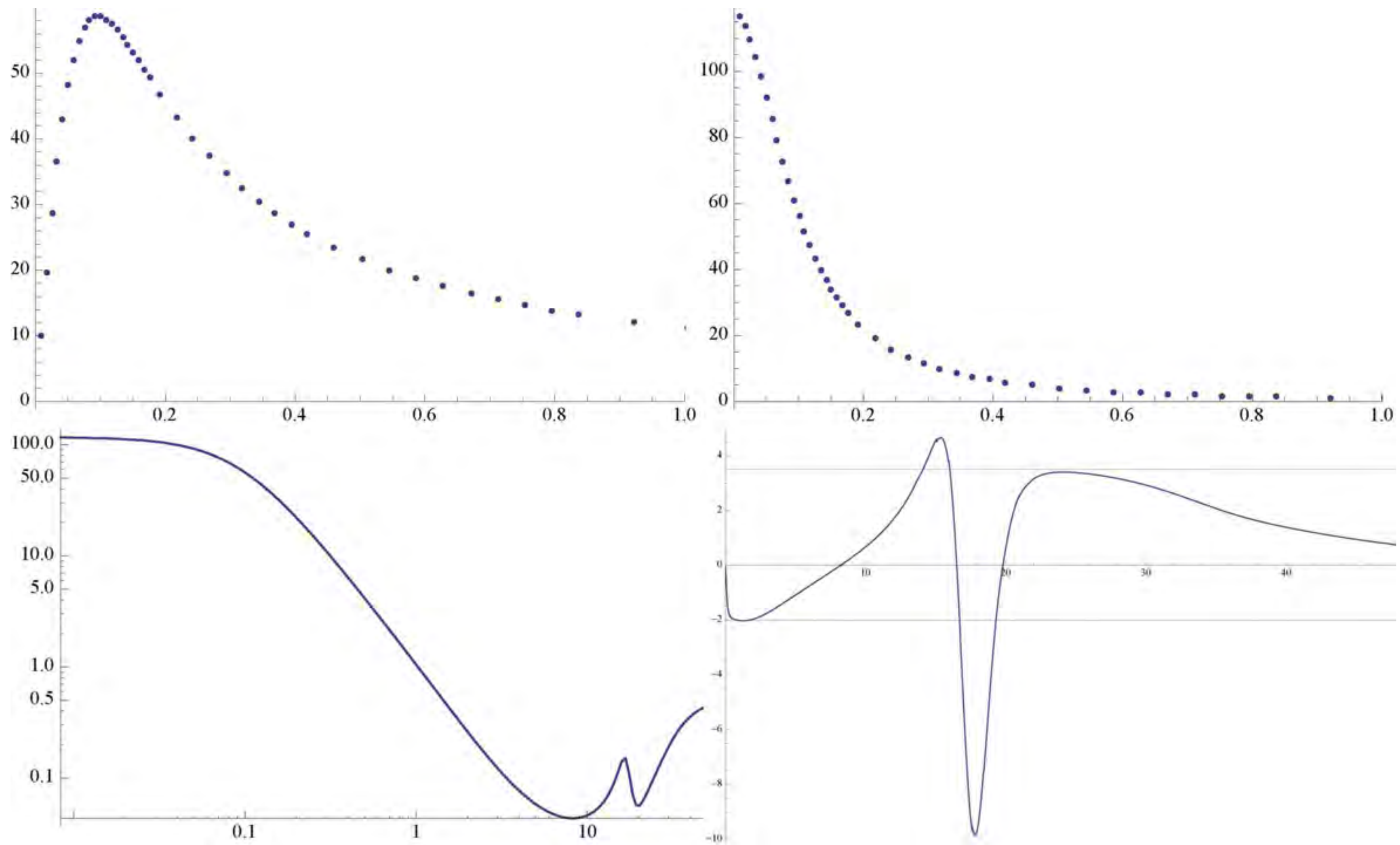

Up left: $Im\ \sigma(\omega)$ vs ω/T Drude peak region. Up right: $Re\ \sigma(\omega)$ vs ω/T Drude peak region. .

Down left: $Re\ \sigma(\omega)$ vs ω/T in log-log plot with the lattice-charge bound state.

Down right: $\frac{d \log Re\ \sigma(\omega)}{d log\omega}$ vs ω/T with the three scaling regimes ω^{-2}, $\omega^{2+\lambda}$, ω^{0}. $k_L/\mu = 2/3$.

Conductivity:$\lambda = 2$

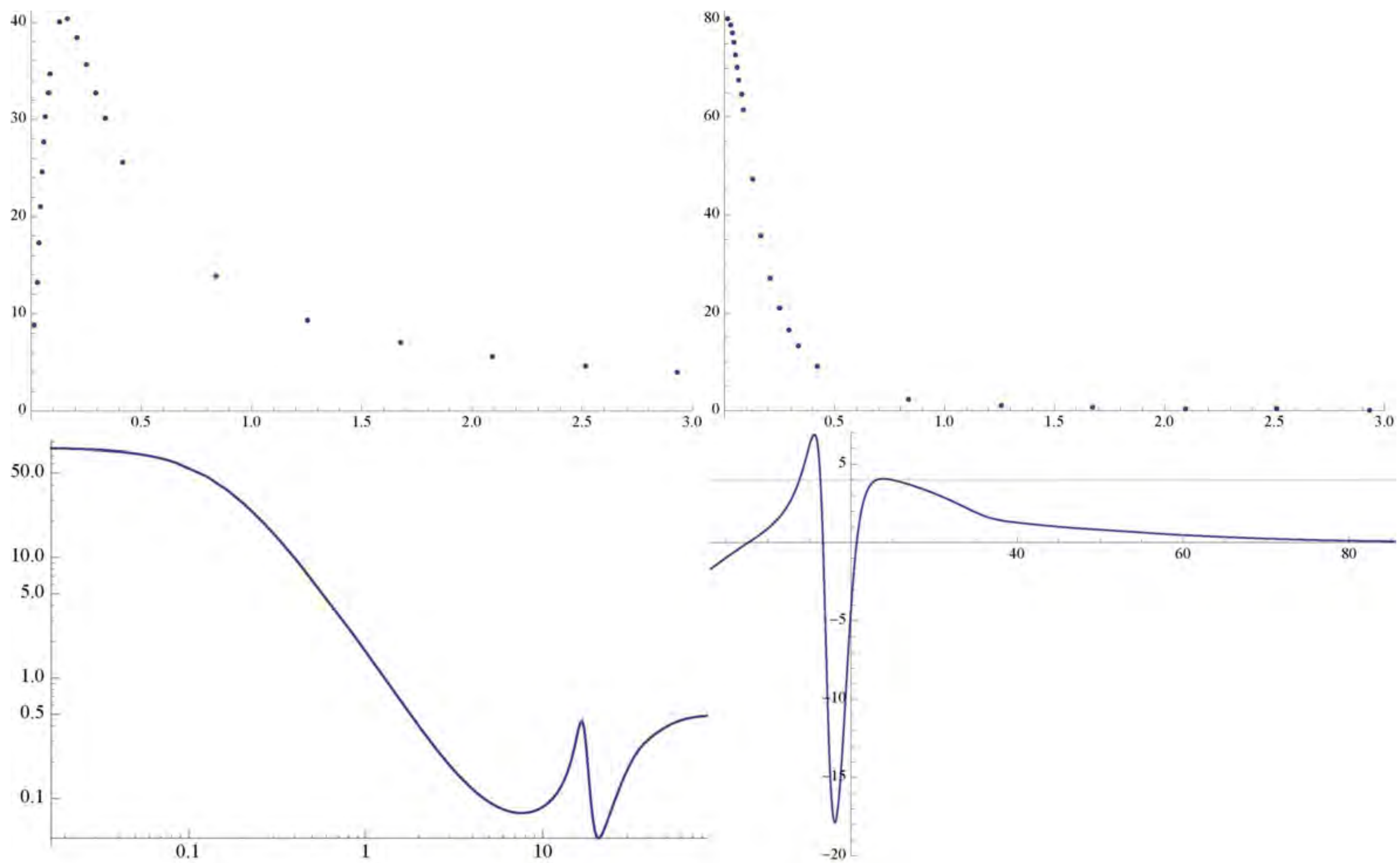

Up left:$Im\ \sigma(\omega)$ vs ω/T Drude peak region. Up right: $Re\ \sigma(\omega)$ vs ω/T Drude peak region. . Down left: $Re\ \sigma(\omega)$ vs ω/T in log-log plot with the lattice-charge bound state. Down right: $\frac{d\log Re\ \sigma(\omega)}{dlog\omega}$ vs ω/T with the three scaling regimes ω^{-2}, $\omega^{2+\lambda}$, ω^{0}.

The DC resistivity

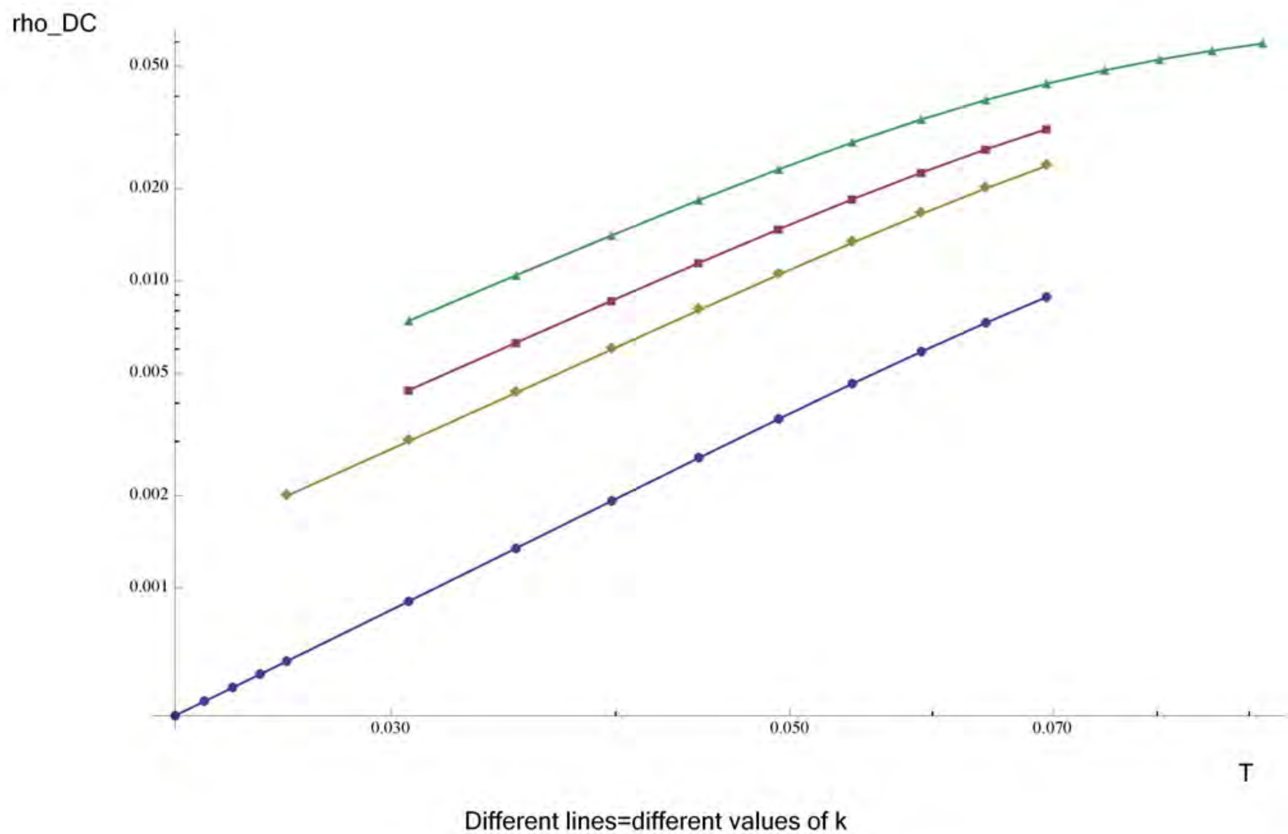

$\log(\rho_{DC})$ vs $\log T$ for different values of k_L^2/μ^2.Prediction:

$$\nu = \frac{\lambda+1}{2\sqrt{\lambda+2}}\sqrt{\lambda+10+4(\lambda+2)k_L^2\ell_{IR}^2 - 8\sqrt{1+(\lambda+2)k_L^2\ell_{IR}^2}}$$

Anantua+Hartnoll+Martin+Ramirez, '12

Temperature dependence

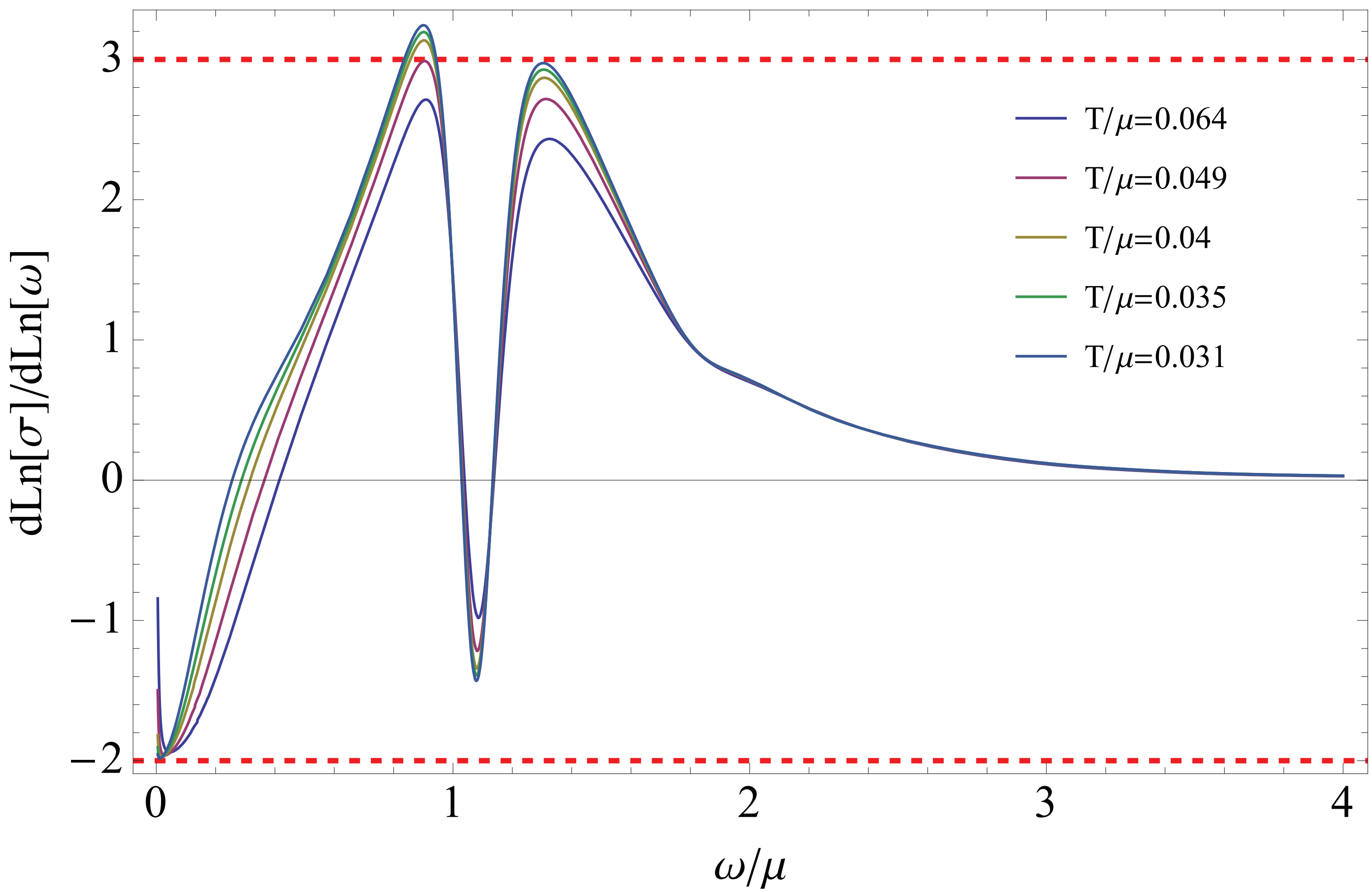

Temperature dependence of the power of $Re\ \sigma(\omega)$ for $\lambda = 1$. There are three regions to observe. The first: $Re\ \sigma \sim \omega^{\lambda+2}$ (UV of AdS_2^{λ}). The second, $Re\sigma \sim \omega^{-2}$ in the Drude peak. The third $Re\sigma \sim \omega^0$ (UV→AdS_4).

The lattice-charge bound-state

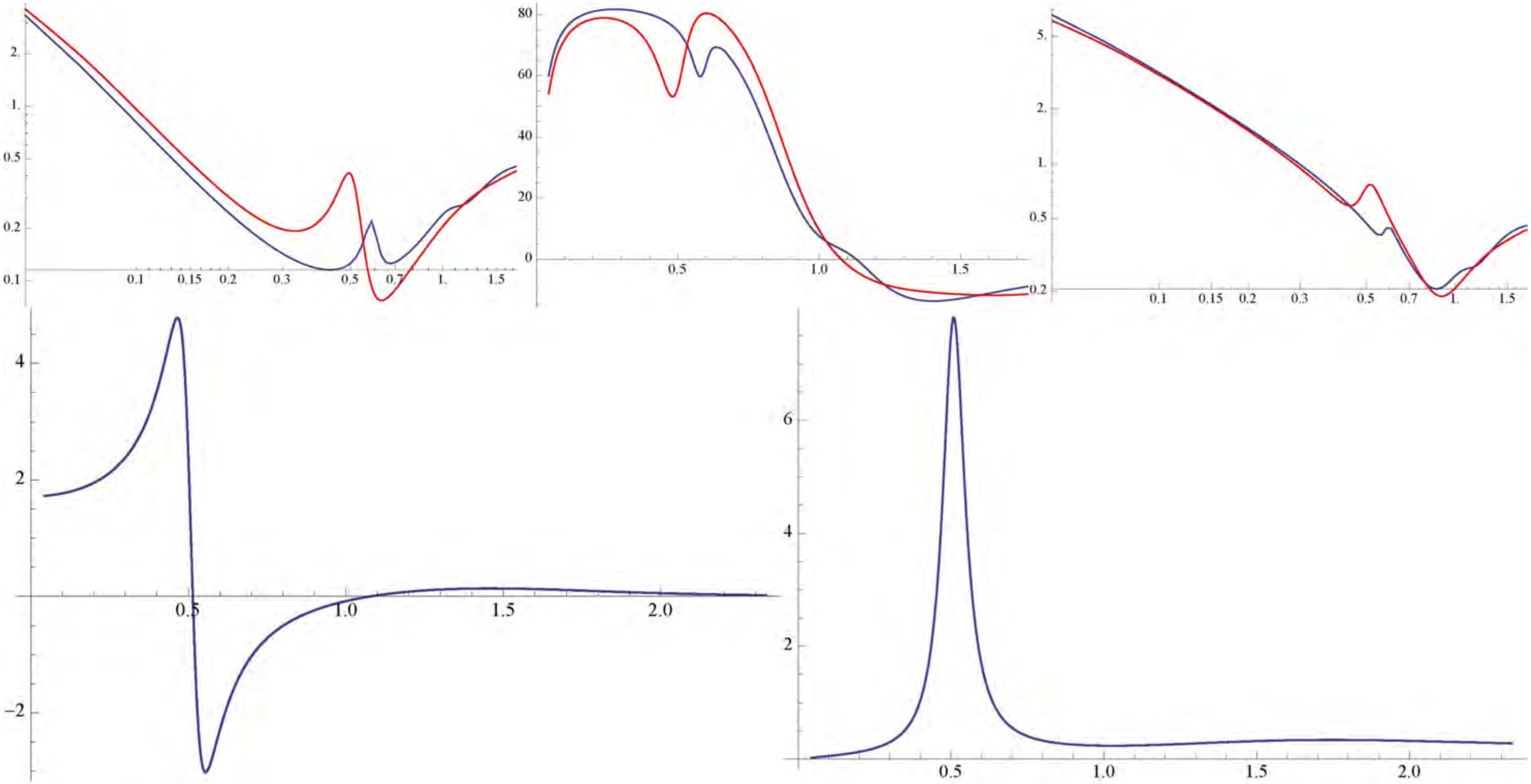

Up left: $|\sigma(\omega)|$ vs ω/μ. Up middle: $Arg(\sigma(\omega))$ vs ω/μ. Up right: $Re\ \sigma(\omega)$ vs ω/μ.

Red line: $A_t = \mu(1 + A\cos(k_L x_1))$. Blue line: $A_t = \mu(1 + A\cos(k_L x_1) + 2A\cos(2k_L x_1))$

Down left: $Re\ \langle J_t J_t \rangle(\omega, k_1 = k_L)$ Down right: $Im\ \langle J_t J_t \rangle(\omega, k_1 = k_L)$ backround: RN.

IR localization

• Another idea to break translation invariance but avoid PDEs is to introduce further symmetry. An example is Bianchi VII_0 (helical symmetry) with invariant forms

Iizuka+Kachru+Kundu+Narayan+Sircar+Trivedi, '12

$$\omega_1 = \mathrm{d}x_1\,, \omega_2 = \cos(kx_1)\mathrm{d}x_2 + \sin(kx_1)\mathrm{d}x_3\,, \omega_3 = \sin(kx_1)\mathrm{d}x_2 - \cos(kx_1)\mathrm{d}x_3$$

• Donos+Hartnoll used an action with two U(1)'s

$$S = \int d^5x\sqrt{g}\left[R + \frac{12}{\ell^2} - \frac{1}{4}F_1^2 - \frac{1}{4}F_2^2\right] - \frac{\kappa}{2}\int A_2 \wedge F_1 \wedge F_2$$

and sources

$$A_{1t} = \mu \quad , \quad A_2 = h\omega_2$$

• The A_2 "magnetic" field breaks translational invariance in the x_1 direction.

• Three IR solutions were found.

(a) A metallic $AdS_2 \times R^3$ geometry,

(b) a bifurcating unstable scaling geometry

(c) an insulating geometry with a metric breaking both translational and rotational invariance.

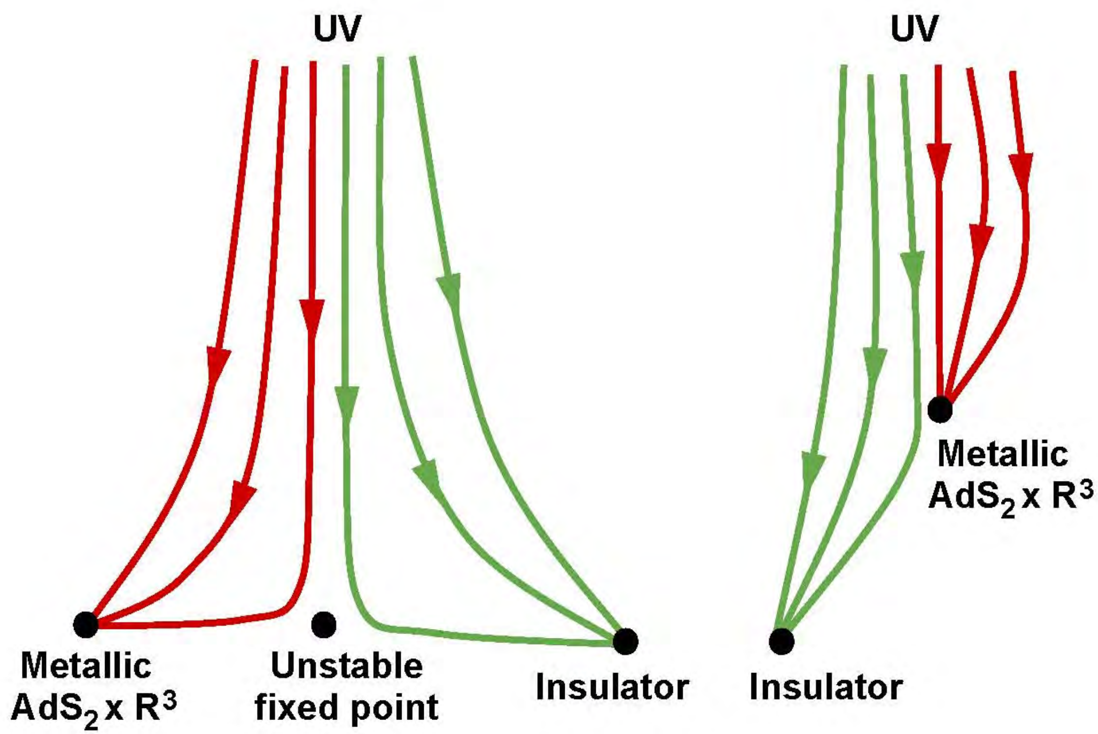

- At $T = 0$,

$$Re\ \sigma_{11} \sim \omega^{\frac{4}{3}} \quad , \quad \omega \to 0$$

Bianchi VII_0 scaling solutions in EM^2D

with Aristos Donos and Blaise Gouteraux

$$S_{EM^2D} = \int d^5x\sqrt{g}\left[R - \frac{1}{2}(\partial\phi)^2 + V(\phi) - \frac{Z_1(\phi)}{4}F_1^2 - \frac{Z_2(\phi)}{4}F_2^2\right]$$

$$V(\phi) \underset{IR}{\sim} V_0 e^{-\delta\phi}, \quad Z_1(\phi) \underset{IR}{\sim} Z_1 e^{\gamma_1\phi}, \quad Z_2(\phi) \underset{IR}{\sim} Z_2 e^{\gamma_2\phi}$$

$$\mathrm{d}s^2 = -D(r)\mathrm{d}t^2 + B(r)\mathrm{d}r^2 + C_1(r)\omega_1^2 + C_2(r)\omega_2^2 + C_3(r)\omega_3^2 \quad , \quad \phi(r)$$

$$A_1 = A_1(r)\mathrm{d}t\,, \quad A_2 = A_2(r)\omega_2$$

The scaling solutions are in general characterized by 6 critical exponents:

$$ds^2 = r^{\frac{2\theta}{3}}\left(\frac{dt^2}{r^{2z}} + B_0\frac{dr^2}{r^2} + \frac{dx_1^2}{r^2}\right) + \frac{\left(\omega_2^2 + \lambda\ r^{\theta_{23}}\omega_3^2\right)}{r^{2z_{23}}}\,,\ A_1 \sim r^{\zeta_1 - z}\,,\ A_2 \sim r^{\zeta_2 - z_{23}}$$

- Parameters: three from the action $(\gamma_1, \gamma_2, \delta)$. Three from the sources (μ_1, h_2, k)

• We have classified all scaling solutions, generic and non-generic. They fall in the following broad classes:

0. Translationally invariant solutions. There are many different kinds. We will not discuss them.

1. Solutions with $\theta_{23} = 0$. They are non-trivial solutions but keep the structure of the plane (x_2, x_3) intact. There many district classes.

2. Solutions with $\theta_{23} \neq 0$. The Donos-Hartnoll (DN) insulator is one of these.

• There several distinct classes.

• Some of them are DH insulators (but with more general exponents)

• Some are "bad metals" $\lim_{\omega \to 0} \quad Re\ \sigma_{11}(\omega, T = 0) \to \infty$

$\theta_{23} = 0$

1.1 Helical solutions with a constant "magnetic field" ($\zeta_2 = z_{23}$).

• There are three distinct sub-classes depending on whether the electric field F^1_{rt} is zero, subleading or leading compared to the rest.

• All of these solutions are translationally non-invariant along x^1.

1.2 Semilocal hyperscaling-violating solutions.

• There are two classes: leading magnetic field, or subleading magnetic field.

• In both cases the metric is translation invariant.

1.3 A generic solution with general exponents, and nontrivial electric and magnetic fields.

$\theta_{23} \neq 0$

- There are three major classes: leading scaling magnetic field, constant magnetic field, and subleading magnetic field.

- The second class has 4 distinct subcases

- For all solutions here we will parametrize the metric and A_1 as

$$ds^2 = r^{\frac{2\theta}{3}} \left[-\frac{\mathrm{d}t^2}{r^{2z}} + L^2 \frac{\mathrm{d}r^2}{r^2} + r^{\beta}\omega_1^2 + r^{-\frac{4}{3}} \left(\omega_2^2 + \lambda r^{\beta} \omega_3^2 \right) \right], \quad A_1 = Q_0 r^{\zeta - z}$$

- The IR entropy scales for all solutions as

$$S \sim T^{\frac{\frac{4}{3} - \theta - \beta}{z}}$$

- We will focus on one of the 6 classes.

New IR geometries

$$\mathrm{d}s^2 = r^{2\frac{\theta}{3}}\left(\frac{L^2\mathrm{d}r^2 - \mathrm{d}t^2}{r^2} + r^{\beta}\omega_1^2 + r^{-4/3}\left(\omega_2^2 + r^{\beta}\omega_3^2\right)\right)$$

$$A_1 = Q_0 r^{\zeta-1}\mathrm{d}t\,, \quad A_2 = \sqrt{\frac{1}{2}(4+3\beta)}\omega_2\,, \quad e^{\phi} = r^{\sqrt{\frac{8}{9}-2\theta+\frac{2\theta^2}{3}-\frac{2\beta}{3}-\beta^2}}$$

- $z = 1$ and the is an AdS_2 part in the metric. There are three free exponents.

- The helical step k is fixed in terms of the parameters (θ, β, ζ).

- We can compute analytically all critical exponents of perturbations around the solution and decide when it is RG stable (no relevant perturbations).

- We can impose also all physicality constraints (Gubser bound, null energy condition, etc).

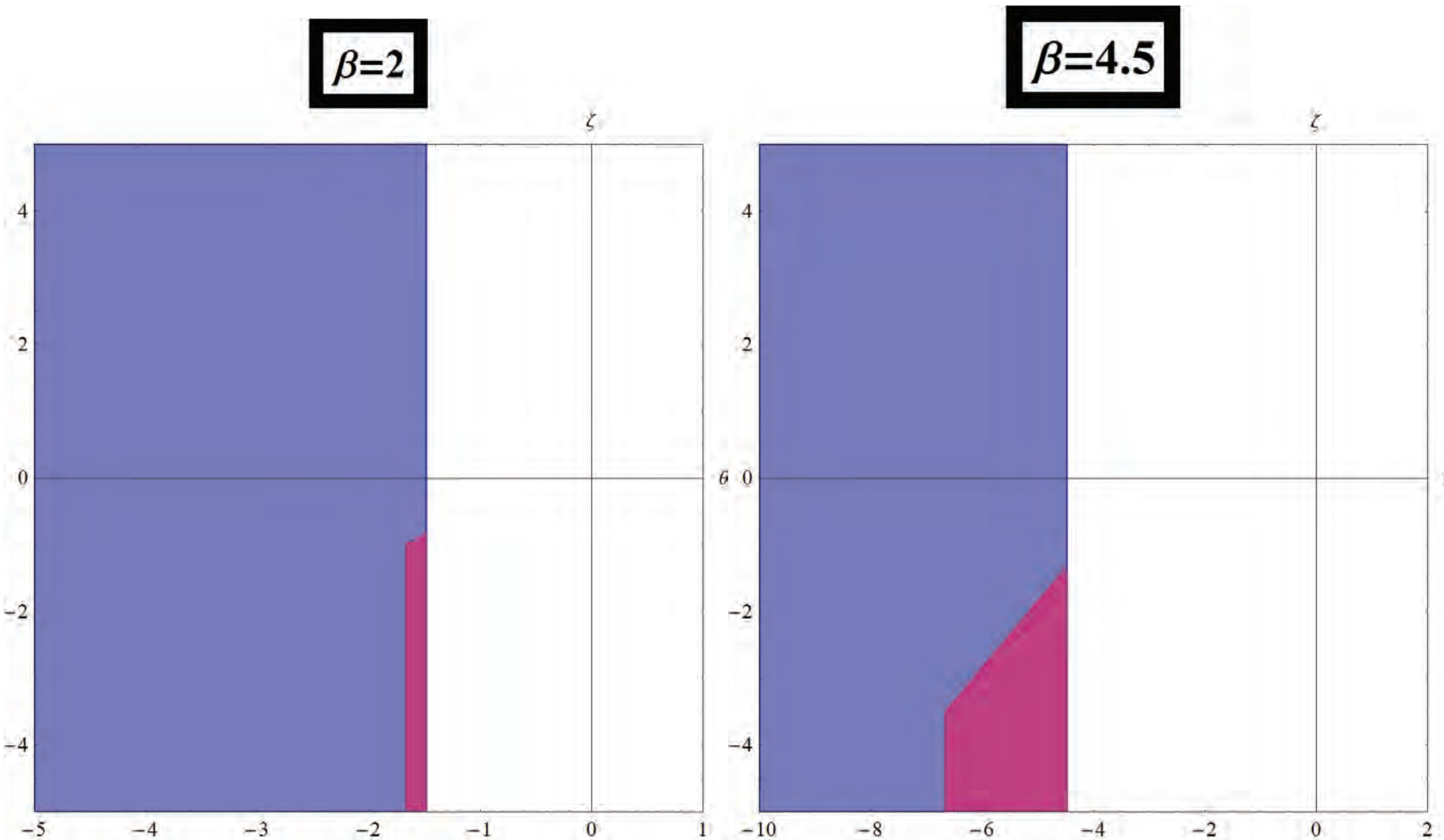

- Blue region: physical solution
- Fuchsia region: RG stable (no relevant perturbations)

Conductivity

- To calculate σ_{11} we must perturb the solution

$$\delta A_1 = e^{-i\omega t} b_1(r) \omega_1 \quad , \quad \delta A_2 = e^{-i\omega t} b_2(r) \omega_3$$

$$\delta(ds^2) = e^{-i\omega t}\left[g_1(r) dt \otimes \omega_1 + g_2(r) \omega_2 \otimes \omega_3\right]$$

- There are four second-order coupled equations for the 4 functions plus one first order constraint.

- They can be diagonalized sequentially, and we can compute the IR asymptotics of the relevant two point functions

$$\text{Im}\, \mathcal{G}^R_{b_1} \propto \omega^{|-1+\zeta+\beta|} \quad , \quad \text{Im}\, \mathcal{G}^R_{\theta} \propto \omega^{\frac{1}{3}\sqrt{\left(\theta-\frac{31}{3}\right)\left(\theta-\frac{7}{3}\right)-8\beta}} \quad , \quad \text{Im}\, \mathcal{G}^R_{\Sigma} \propto \omega^{\left|\frac{13}{3}-\theta\right|}$$

and

$$Re\sigma_{11} \sim C_{b_1} \frac{\text{Im}\, \mathcal{G}^R_{b_1}}{\omega} + C_\theta \frac{\text{Im}\, \mathcal{G}^R_{\theta}}{\omega} + C_\Sigma \frac{\text{Im}\, \mathcal{G}^R_{\Sigma}}{\omega}$$

- We must find the smallest of these exponents, and this determines the DC conductivity at zero temperature.

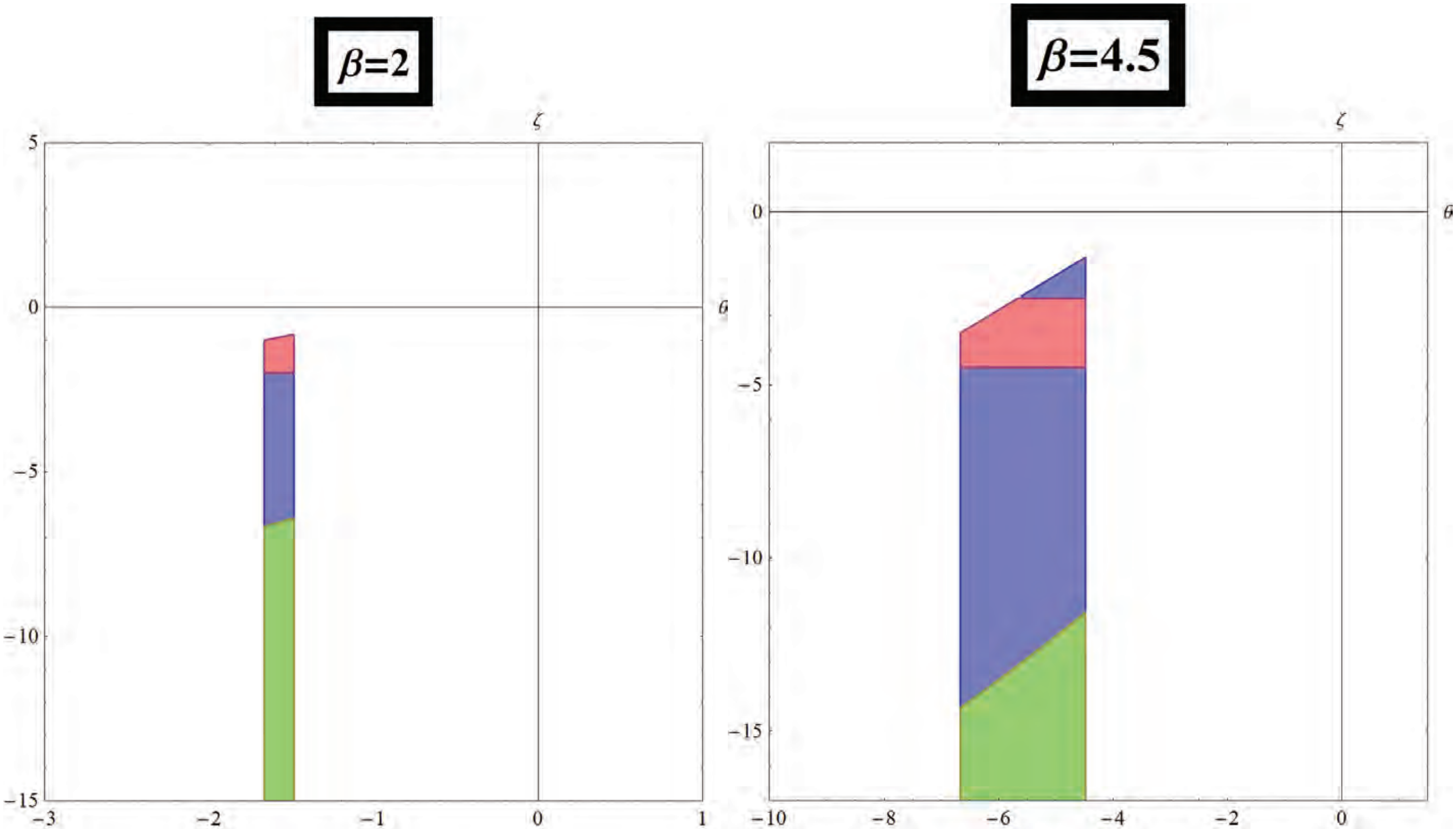

Blue region: σ_{b_1} dominates with a positive power, $\rightarrow$ insulator.
red region: σ_{b_1} dominates with a negative power, $\rightarrow$ bad metal.
green region: σ_{Σ} dominates with a positive power, $\rightarrow$ insulator.

- In the transition regions we expect new phenomena to happen.

Outlook

Many issues remain to be cleared up:

• In the hyperscaling-violating geometries, the conductivity for all hyper-scaling violating geometries with lattices remains to be computed.

• The resolution of the $\delta(\omega)$ for the gapped hyperscaling geometries remains to be done.

• The new helical geometries producing insulators and bad metals must be analyzed further, and incorporated in complete RG flows.

• The many other solutions found remain to be characterized.

• We expect that similar EM^2D solutions must exist with non-Bianchi type translational breaking, but they should be found numerically.

• The global stability of such solutions should be studied.

Quantum Field theory, String Theory and Condensed Matter Physics

Home | Program | Information | Participants | Travel | The region

1-7 September 2014

(31 August is arrival day, 8 August is Departure day)

International Organizing Committee	Local Organizing Committee
• Costas Bachas (Paris) • Koenraad Schalm (Leiden) • David Tong (Cambridge) • Jan Zaanen (Leiden)	• Elias Kiritsis (UoC) • Vassilis Niarchos (UoC) • Christos Panagopoulos (UoC) • Giorgos Tsironis (UoC)

.

THANK YOU

Solutions at zero charge density

.

Gursoy+Kiritsis+Mazzanti+Nitti (2009)

• The only parameter relevant for the solutions is $\delta \in R$ in $V \sim e^{-\delta\phi}$. Take $p+1=4$.

• $0 \leq |\delta| < 1$. T=0 singularity acceptable. Continuous spectrum/no mass gap. Continuous transition to BH phase at $T > 0$

• $1 < |\delta| < \sqrt{3}$. Discrete spectrum/mass gap. BH is thermodynamically subdominant and unstable. $1 < |\delta| < \sqrt{\frac{5}{3}}$. The spin-2 and spin-0 spectral problem is reliable without resolution.

• $|\delta| \geq \sqrt{3}$. Gubser bound violated, singularity→unacceptable.

The crossover value here is $|\delta| = 1$. For all other $\delta \neq 1$, corrections like $V = e^{-\delta\phi}\phi^k + e^{-\delta'\phi}\phi^{k'} + ...$ give subleading corrections.

- $1 < |\delta| < \sqrt{3}$. In the gapped case, the BH is unstable and thermodynamically irrelevant. The complete story at finite T depends on the subleading terms in the potential (aka the UV completion).

- There is a first order phase transition at T_c to a large BH.

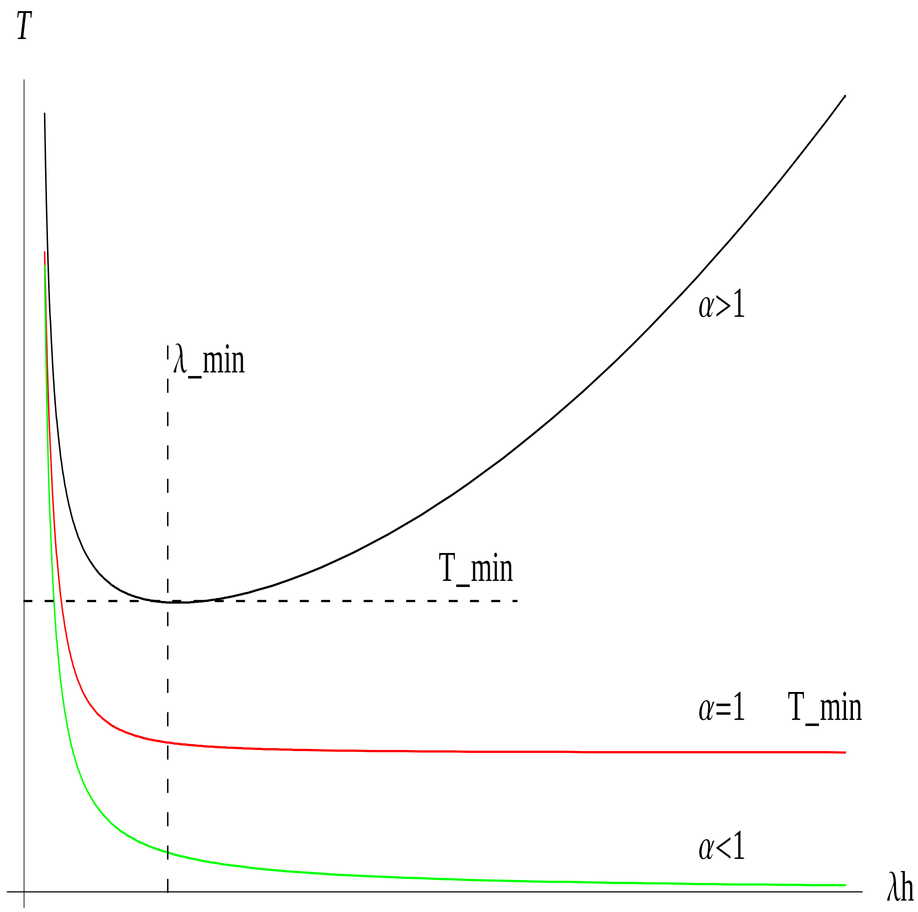

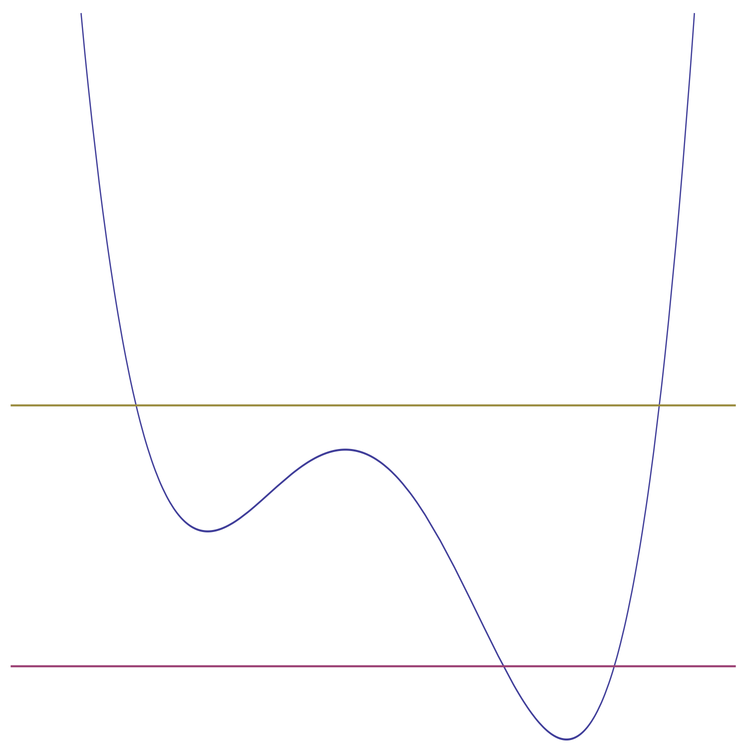

- For more complicated potentials multiple phase transitions are possible.

Gursoy+Kiritsis+Mazzanti+Nitti (2009), Alanen+Kajantie+Tuominen (2010)

• $|\delta| = 1$. This is the "marginal" case. It has a good singularity, a continuous spectrum and a gap. A lot of the physics of finite temperature transitions depends on subleading terms in the potential:

♠ If $V = e^{\phi}\left[1 + C\, e^{-\frac{2\phi}{n-1}} + \cdots\right]$, then at $T = T_{min} = T_c$ there is an n-th order continuous transition.

♠ If $V = e^{\phi}\left[1 + C/\phi^k + \cdots\right]$, then at $T = T_{min} = T_c$ there is a generalized KT phase transition

Gursoy (2010)

♠ If $V = e^{\phi}\ \phi^P$, with $P < 0$ this behaves as in $|\delta| < 1$. When $P > 0$ like $|\delta| > 1$.

The spectra depend importantly on P, when $P > 0$.

In particular, we will see that $P = \frac{1}{2}$ is very much like what we expect in 4D large-N YM.

Charged near-extremal scaling solutions

$$ds^2 = r^{\frac{(\gamma-\delta)^2}{2}}\left[dx^2 + dy^2 - f(r)dt^2\right] + \frac{dr^2}{f(r)}$$

$$f(r) = \frac{16\,(-\Lambda)}{wu^2}e^{-\delta\phi_0}\quad r^{1-\frac{3}{4}(\gamma-\delta)^2+\frac{wu}{4}}\quad\left(1-\frac{2m}{r^{\frac{wu}{4}}}\right),$$

$$e^{\phi} = e^{\phi_0}r^{-(\gamma-\delta)}\quad,\quad \mathcal{A} = \frac{8}{wu}\sqrt{\frac{v\Lambda}{u}}e^{-\frac{(\gamma+\delta)}{2}\phi_0}\quad\left[r^{\frac{wu}{4}} - 2m\right]dt$$

$$wu = 3\gamma^2 - \delta^2 - 2\gamma\delta + 4 > 0\,,\quad u = \gamma^2 - \gamma\delta + 2\,,\quad v = \delta^2 - \gamma\delta - 2\,,\delta^2 \le 3$$

- These are near extremal solutions (the charge density is fixed).
- The Entropy vanishes at extremality if $\gamma \neq \delta$.
- If $\gamma = \delta$ the extremal solution is $AdS_2 \times R^2$.
- The charge entropy dominates the $Q = 0$ entropy almost everywhere.
- When $\frac{dS}{dT} < 0$ the BH is unstable$\to$ gapped spectra.

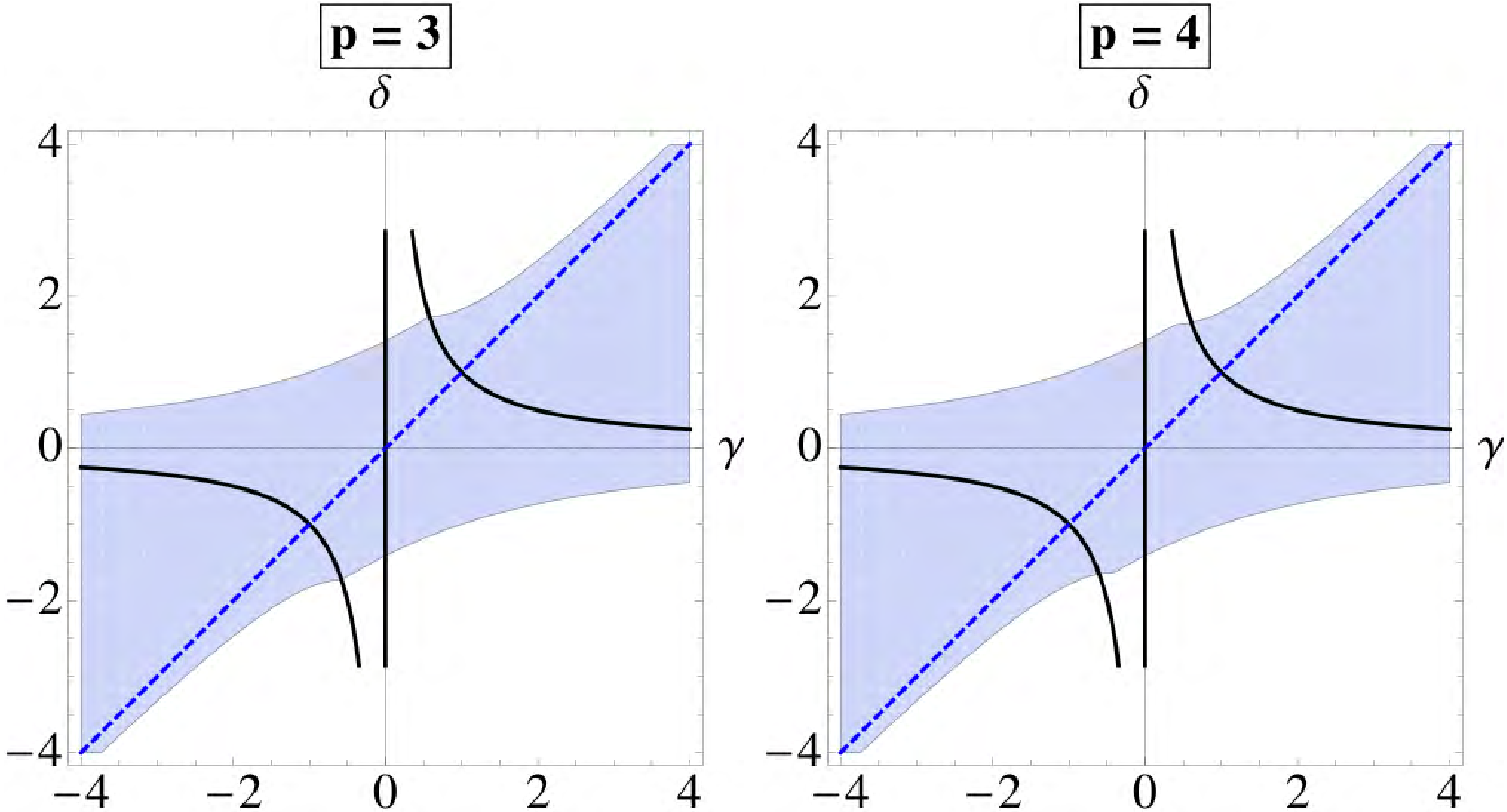

This graph shows the Gubser bounds on the near extremal solution on the whole of the (γ, δ) plane for $p = 3$ and $p = 4$. The blue regions are the allowed regions where the near extremal solutions are black-hole like. The white regions are solutions of a cosmological type and therefore fail the Gubser bound. The dashed blue line is the $\gamma = \delta$ solutions while the solid black line corresponds to the $\gamma\delta = 1$ solutions.

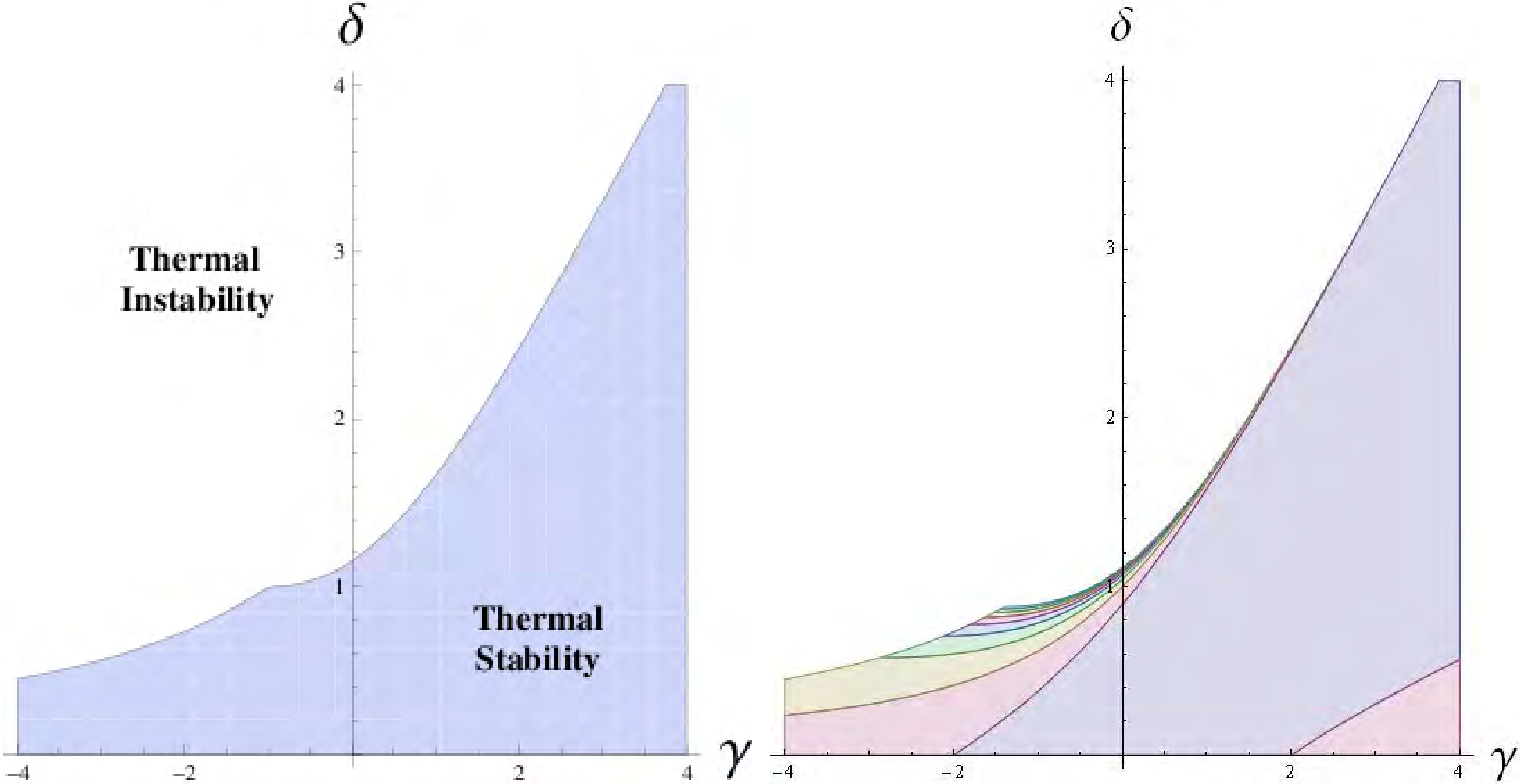

On the left: region of local stability of the near extremal black hole. Right: The variety of phase transitions of the near extremal black hole to the background at zero temperature. In the blue region continuous transitions occur, in the purple region adjacent to the blue one the transitions are of third-order. The stripes starting with yellow to the left of the blue and purple regions depicts transitions of fourth-(yellow) up to tenth-order. Above them all higher-order transitions also occur.

Symmetries

• In HEP the basic symmetry required is Poincaré invariance that together with scaling leads (usually) to conformal invariance.

In non-relativistic frameworks (condensed matter) several reductions are possible

• Give up Boosts

• Give up translation invariance

• Give up rotations

• Allowing Lifshitz scaling symmetries

• Allowing more complex symmetries like Schrödinger symmetries.

Critical lines vs critical points in Cuprates

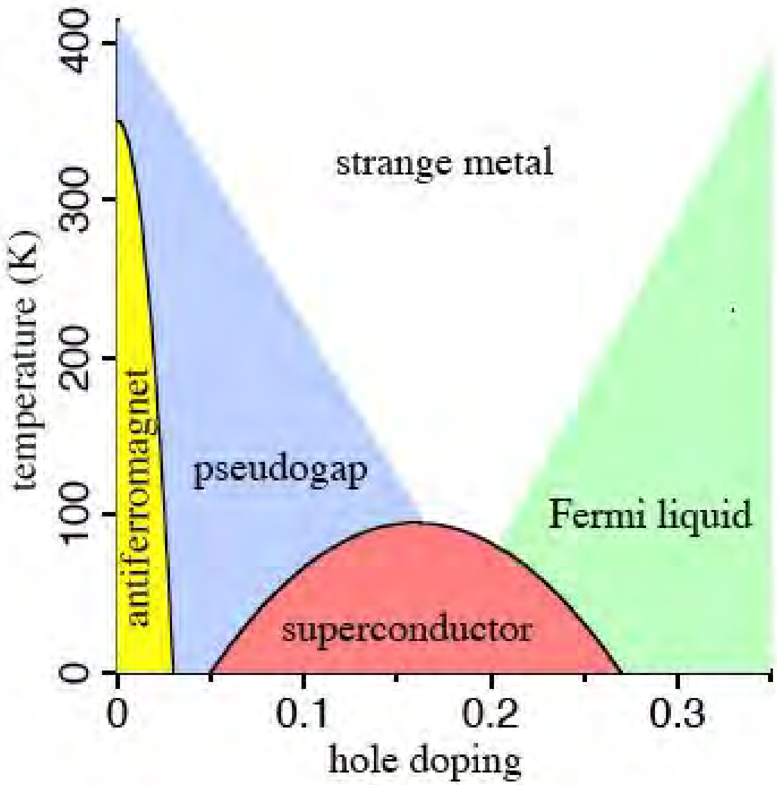

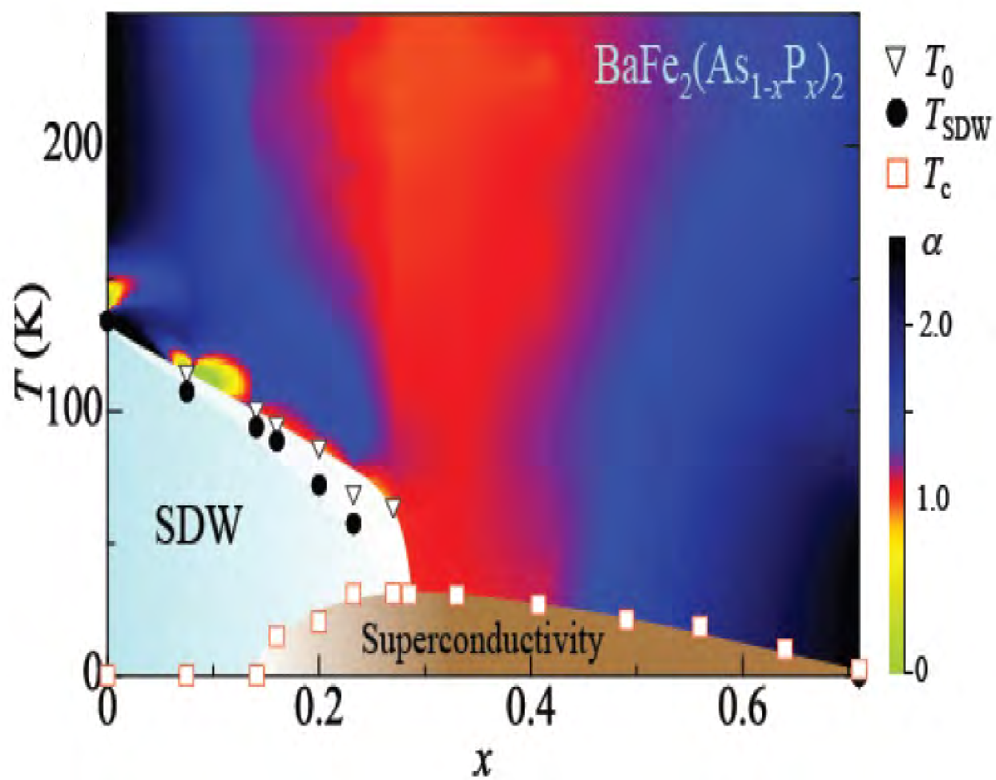

$$H = \Sigma_{\langle ij \rangle} \; J_{ij} \; \vec{S}_i \cdot \vec{S}_j$$
$$J, J/g \to J_{ij} \quad , \quad g > 1$$

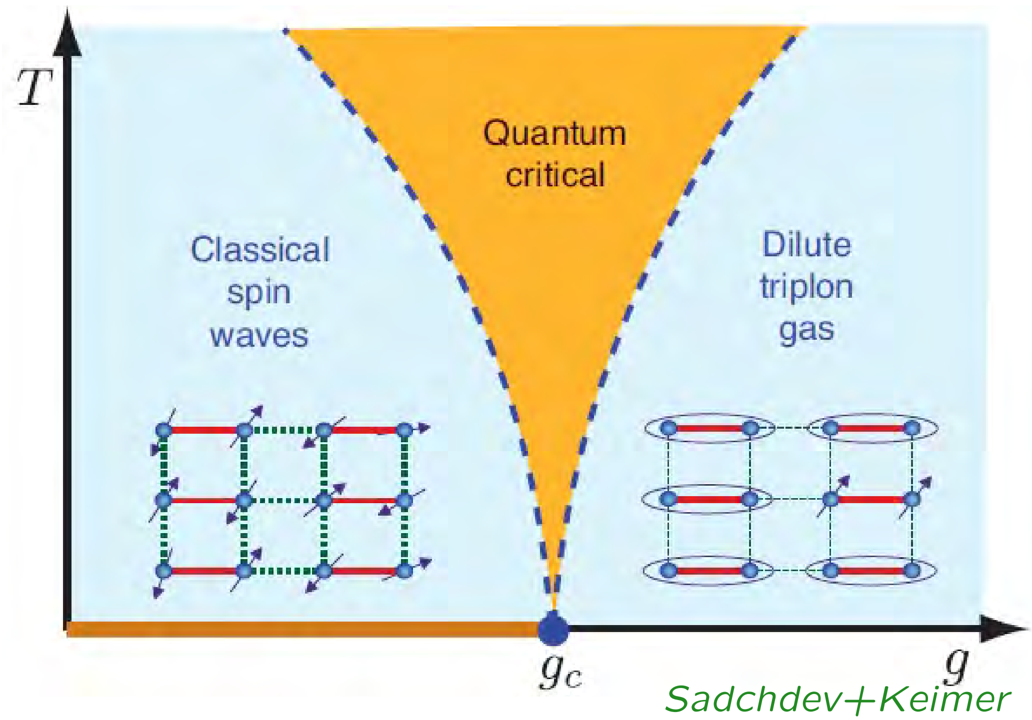

- Quantum phase transition at T=0
- Critical cone above.

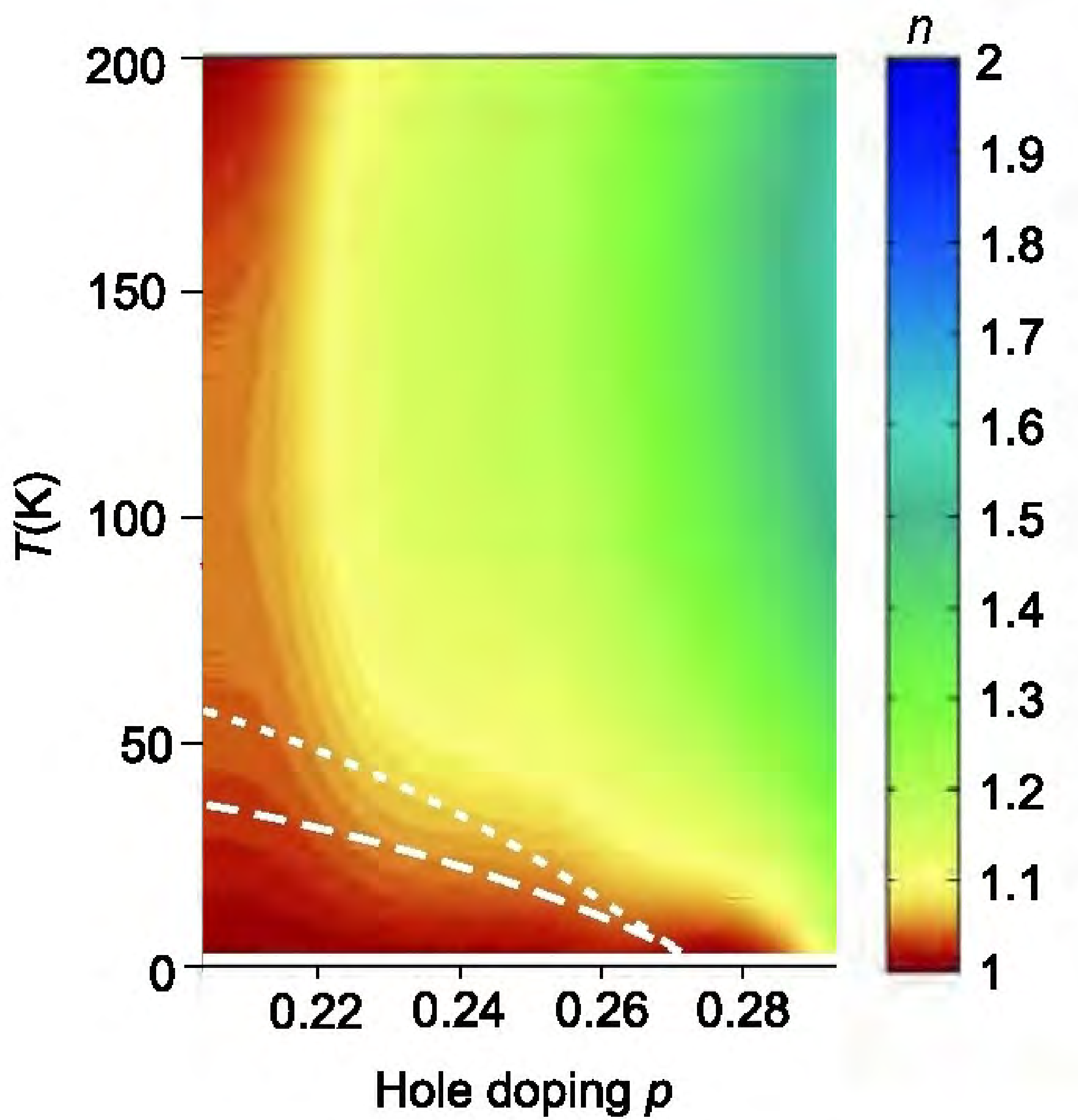

Anomalous Criticality in the Electrical Resistivity of $La_{2-x}Sr_xCuO_4$.

R.A. Copper et. al. 2009

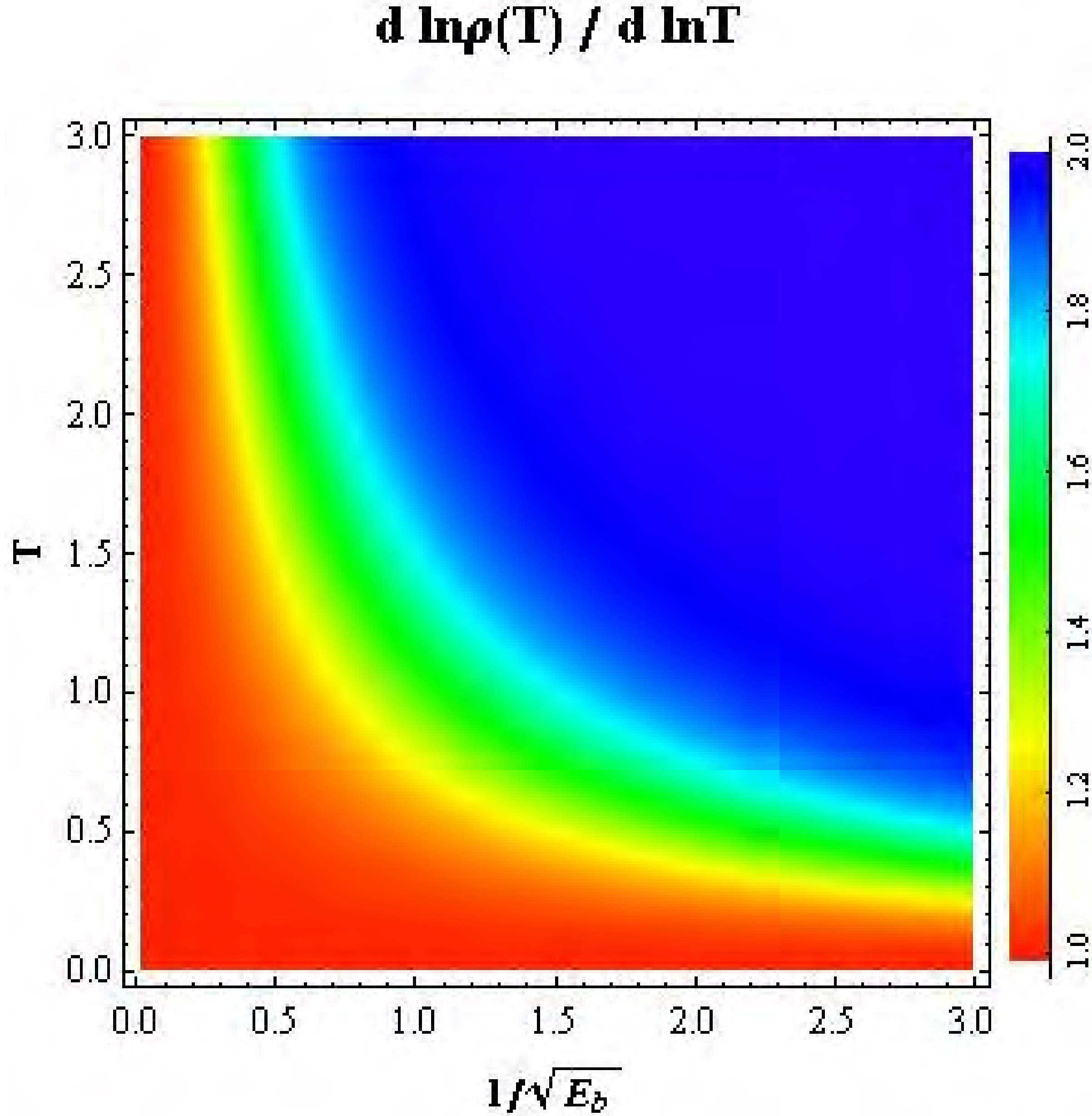

Kim+E.K.+Panagopoulos

Detailed plan of the presentation

- Title page 0 minutes
- Bibliography 0 minutes
- The plan 1 minutes
- Introduction 3 minutes
- Fixed Point Theories 5 minutes
- Classification of QC theories 6 minutes
- Important characteristics of Saddle-points 7 minutes
- Fractionalized vs cohesive phases 10 minutes
- Quantum fractionalisation transitions 11 minutes
- Conductivity 15 minutes
- Insulators at Strong Coupling 17 minutes
- Discrete Current-Current Spectra 18 minutes
- Conductivity in semilocal geometries 21 minutes
- Convergence 22 minutes

- The backgrounds 25 minutes
- Conductivity:$\lambda = \frac{3}{2}$ 27 minutes
- Conductivity:$\lambda = 2$ 28 minutes
- Temperature dependence 29 minutes
- The charge-lattice bound state 31 minutes
- The DC resistivity 33 minutes
- IR localization 36 minutes
- Bianchi VII_0 scaling solutions in EM^2D 40 minutes
- $\theta_{23} = 0$ 41 minutes
- $\theta_{23} \neq 0$ 42 minutes
- New IR geometries 45 minutes
- Conductivity 48 minutes
- Outlook 49 minutes

- Symmetries 50 minutes
- Solutions at Zero Charge Density 56 minutes
- Charged near extremal solutions 60 minutes
- Critical lines vs critical points 63 minutes